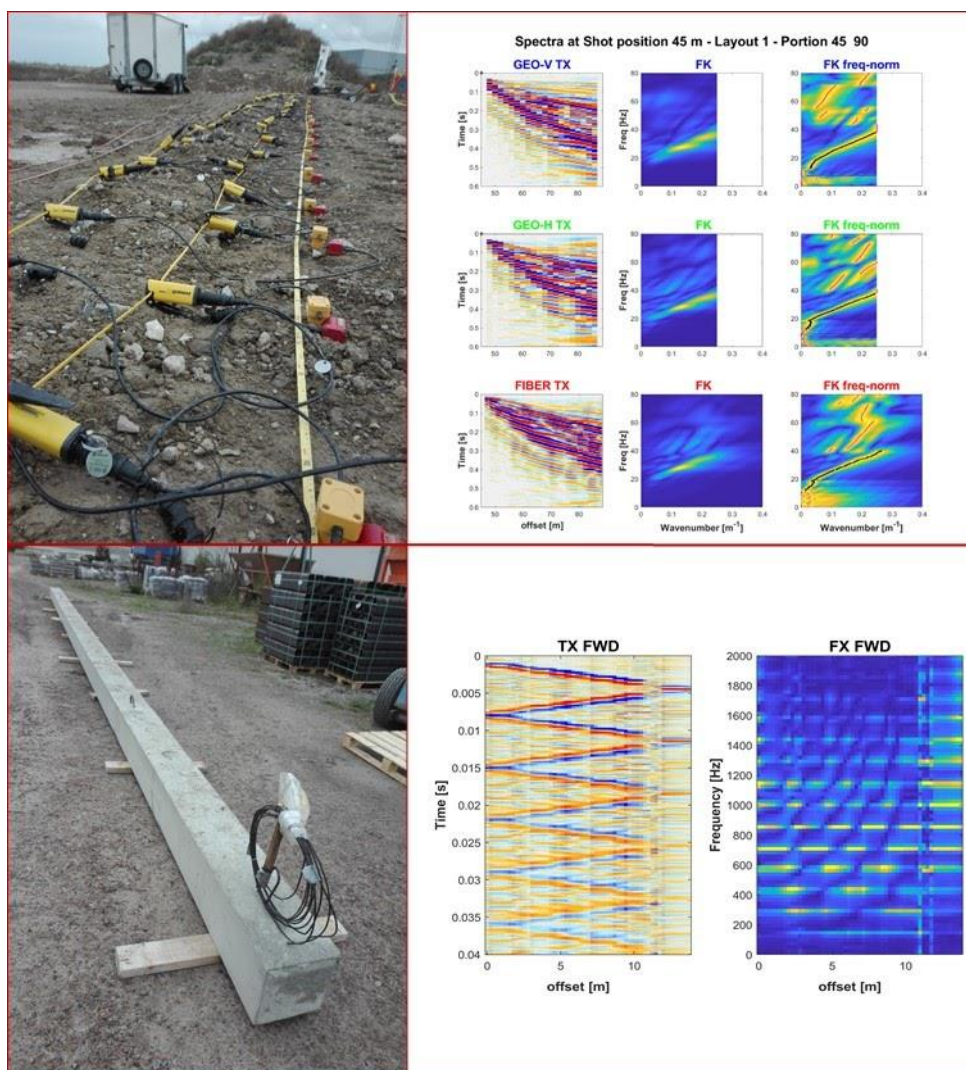


KONTROLL AV MARKSTABILISERING MED OPTISK FIBER



Matteo Rossi, Roger Wisén och Nils Rydén

2020-10-05

FÖRORD

Detta projekt har utförts under 2018, 2019 och 2020 på avdelningen för Teknisk Geologi (Lunds Tekniska Högskola, Lunds Universitet) med finansiering från SBUF (Svenska Byggbranschens Utvecklingsfond) genom Peab och Vinnova (id: 2018-00641). Matteo Rossi och Roger Wisén är huvudförfattare till slutrapporten och har utfört alla seismiska mätningar och analys av data. Nils Rydén deltog i betongpåletestet, genom planering, mätning, och i diskussionen om resultat.

Vi tackar:

- deltagare av projektet Hydroresearch AB, Silixa ltd, PEAB AB och Skanska Sverige AB för stöd till projektet.
- SGI och NCC som medlemmarna i referensgruppen.
- särskilt Peab Grundläggning AB (Tollarp, Sweden) för att hjälpa oss med pelartestet;
- särskilt Skanska Sverige AB för stöd att ESS byggarbetsplats.
- Professor Giulio Vignoli (Department of Civil and Environmental Engineering and Architecture, University of Cagliari, Italy) för inversion av ytvågor.

Matteo Rossi, Roger Wisén (Teknisk Geologi, Lunds Universitet)
och Nils Ridén (Peab Anläggning AB),
2021-03-24

SAMMANFATTNING

Markstabilisering blir allt vanligare för exploatering av områden med dålig bärighet då det leder till stora ekonomiska besparingar jämfört med alternativa metoder. Markstabilisering är också mycket fördelaktigt ur ett miljö- och hållbarhetsperspektiv då det minimerar transporter och sparar natur-resurser. Detta är indirekt kopplat till riksdagens miljömål vad gäller klimatmålen. För att bättre leva upp till miljömålen måste användandet av restprodukter öka. Detta ställer nya och ökade krav på kvalitetsuppföljning. Det finns dock ett stort behov av bättre och volymstäckande kontrollmetoder för kvalitetssäkring.

Kontrollen kan delas upp i två steg, där det första ska ske i omedelbar anslutning till inblandning av bindemedel för att kontrollera om man lyckats behandla hela den avsedda volymen, eller om det finns zoner som behöver komplettering. Det andra steget har fokus på kontroll av hållfasthetstillväxten, och kan inte göras förrän tillräcklig härdning har skett. Detta projekt har fokus på det andra steget och baseras på seismiska metoder med optisk fiber (DAS) som sensorkabel. Mätning har skett parallellt med traditionella sensorer, för att ge möjlighet att utvärdera upplösning och signal-brusförhållande för respektive mätteknik. Seismisk mätning med optisk fiber är tack vare teknikutveckling nu ett möjligt alternativ till traditionella seismiska sensorer. Den optiska fibern möjliggör också temperaturmätning för ytterligare information om härdningsförloppet. En fördel med optisk fiber som sensor är den låga kostnaden. Då tekniken är oprövad i denna tillämpning behöver test och verifiering av tekniken ske innan det görs försök att tillämpa den i full skala.

Med bättre kontrollmetoder kan man få ökad acceptans för att använda markstabilisering istället för att schakta bort och ersätta material på plats. Därmed kan man spara mer värdefulla råvaror, och undvika deponering och onödiga transporter. Det finns dock ett stort behov av bättre kontrollmetoder. Detta projekt har fokus på kontroll av hållfasthetstillväxten och baseras på seismisk mätning med optisk fiber som sensorkabel. Genom att installera kablarna i konstruktionen öppnar det möjlighet för efterkontroll på ett enkelt och repeterbart sätt vid godtyckliga tillfällen.

Mål för projektet är att undersöka om akustiska mätningar med optisk fiber framgångsrikt kan tillämpas för kontroll av markstabilisering.

Resultaten visar att signalen från fiberoptik är direkt jämförbar med traditionella akustiska (seismiska) mätningar med accelerometer eller geofon.

Resultaten visar att dagens teknik för fiberoptiska sensorer motsvarar en spatial upplösning som motsvarar konventionell mätning med 2 m sensoravstånd. DAS är för närvarande under utveckling och man kan förvänta sig att den spatiala upplösningen snart kan komma att bli bättre (kortare sensoravstånd).

Vi analyserade två fall, ytstabilisering och betongpåle, men vi är övertygade om att metoden också kan vara användbar för undersökning av andra typer av markstabilisering (t.e.x. Masstabilisering).

INNEHÅLL

1. INTRODUCTION AND BACKGROUND	4
2. METHODOLOGY	6
2.1 INSTRUMENTATION	6
2.1.1 Optic fiber Distributed Acoustic Sensing	6
2.1.2 Geode system - London test	7
2.1.3 DMT system - ESS site	9
2.2 PROCESSING	9
2.2.1 Analysis: Time-Space (TX) and Frequency-Wavenumber (FK) domain	10
3. FIELDWORK	11
3.1 PILLAR GOTHENBURG	11
3.2 LONDON TEST	11
3.3 ESS SITE	12
3.4 PILE EXPERIMENT	18
4. RESULTS AND DISCUSSION	21
4.1 LONDON TEST	21
4.2 ESS SITE EXPERIMENT	21
4.3 PILE EXPERIMENT	34
5. CONCLUSIONS	43
6. ACKNOWLEDGEMENTS	44
7. REFERENCES	44

1. INTRODUCTION AND BACKGROUND

Distributed Acoustic Sensing (DAS) is a recent development (last decade) of fiber optic technologies. DAS records acoustic waves, measuring the stretching of the fiber optic subjected to elastic vibrations. The majority of the application for this innovative methodology have been focused on deep seismic explorations, mainly for the oil and gas sector, due to the low spatial resolution of the technique and the high costs of the instruments under development. As this methodology is consolidating and the technical developments are rapidly advancing towards higher spatial resolutions, DAS opens extensive possibilities for medium/small scale applications in civil and environmental engineering.

The project focus on pilot tests for engineering applications that could largely benefit the DAS technologies. We tested the DAS performance in a strictly civil engineering application, where we explored the possibility of using fiber optics for assessing the quality of soil stabilization procedures via acoustic measurements.

Soil stabilization is an engineering application that faces an increasing demand for exploiting areas with poor bearing capacity. It generally results in large financial savings compared to alternative methods. In many cases, soil stabilization is the only practical and economically viable alternative. Soil stabilization is very attractive from a sustainability perspective regarding natural resources. First of all it is possible to utilize local material that would otherwise become a landfill problem, and secondly it saves valuable raw materials in the form of natural gravel or crushed rock. Utilizing local materials also reduces the need for transporting and hence also contributes to decreasing carbon dioxide emissions.

Soil stabilization can also be used to encapsulate contaminated soil in-situ to prevent dispersion of pollutants, avoiding expensive and environmentally hazardous practices such as excavation, transport, treatment and deposition in a new area. Another advantage of stabilizing contaminated ground in-situ is to avoid dangerous exposures of people that handle the polluted material.

Several engineering solutions might be applied for stabilizing soil:

- *Surface stabilization.* A stabilizing binder is milled into a layer of soil material, usually the shallower decimeters. The method is used to stabilize the shallower portion of the soil e.g. for a road construction or in combination with pillar reinforcement to create a pillar deck.
- *Lime-Cement pillars.* They are produced by lowering down a mixing tool to the desired depth and, while the tool is pulled up with a rotational movement, a dry binder is discharged in the ground. The pillars are usually made in densely spaced rows or grids to create almost continuous walls or blocks.
- *Jet grouting.* The method aims to manufacture cement stabilized pillars by drilling to the planned depth and, while pulling the drill up, injecting a cement suspension under high pressure.

- *Mass stabilization.* A dry binder is mixed into large volumes of soft geological materials, such as clay or peat, to create a stiffer mass.
- *Stabilization and solidification of dredged sediments.* Dredged materials, which are often contaminated, might be mixed with a binder before pumping them in a new area. There are several advantages compared to discharge dredged volumes on landfills. Both landfill fees and transport costs are avoided. Furthermore, the local sediments can turn into a construction material, saving external raw materials and thus economical resources. The decreased demand in material transportation reduces the carbon dioxide emissions.

Regardless of the applied stabilization solution, there is a need for better control methods that are time and cost-effective. They might verify if the final outcome is in accordance with the desired properties of the stabilized volume. The results are dependent by several variables, e.g. the type of soil material, type of binder, heterogeneity in soil composition, technical parameters of the mixing procedure. These uncertainties may lead to inhomogeneities of the final product. For this reason, quality control is essential and can be performed through drilling of cores or excavating entire test columns, which are costly and destructive methods.

The quality control can be divided into two parts. The first consists of checking if the entire volume that is intended to treat has been involved in the stabilization procedure or if supplementary efforts are needed in some portions. This step needs to be accomplished directly after the stabilization, when the material is not stiff yet and remediations could be applied.

Once the binder has hardened, a second stage of quality control is required. Seismic measurements can be applied as non-invasive and non-destructive testing (e.g. Lin et al. 2017; Lindh 2016). Rydén and Lindh (2015) have evaluated non-destructive seismic measurements on jet grouting columns and concluded that there are limitations but also the potential to develop a cost-effective control method. Complementary acquisitions with Vertical Seismic Profiling (VSP), surface wave and refraction seismics are recommended for further developments. One complication is the difficulty of locating sensors in the stabilized volume. An advantage could be the possibility to install sensors in conjunction with the stabilization procedure, but they should have a low cost to leave them permanently in the ground. Optical fibers are a good candidate, thanks to the recent technology developments (Parker et al. 2014). The same optical fiber could also be used for temperature measurements during the first stage.

2. METHODOLOGY

2.1 Instrumentation

All in all measurements have been made with four different setups. A first test was performed in December 2018 at Silixa's facilities in London. These measurements were made with optic fiber using Silixa's intelligent Distributed Acoustic Sensing (iDAS v3) and a conventional seismic setup using a Geometrics Geode and 3-axial 4.5 Hz geophones.

During the main field campaign in September 2019 measurements were made with two different setups. The Carina Sensing System technology, which comprehends an iDAS v3 interrogator and an engineered ("constellation") fiber, was used in all of the tests. The DAS data have been compared with different traditional acoustic measurements according with the different applications. For the acquisitions on a concrete pile we used an accelerometer PCB model 393A03. In the survey on stabilized ground we performed seismic measurements with a DMT SummitX system with 2-axial geophones.

2.1.1 Optic fiber Distributed Acoustic Sensing

Distributed sensing is a technology that enables continuous, real-time measurements along the entire length of a fiber optic cable. Distributed sensing is usually used for acquiring temperature, strain and acoustic data and this project specifically utilizes Distributed Acoustic Sensing (DAS). Unlike traditional sensors that rely on discrete sensors measuring at pre-determined points, distributed sensing does not rely upon manufactured sensors but utilizes the optical fiber. The optical fiber is the sensing element without any additional transducers in the optical path.

The interrogator operates according to a radar-style process: it sends a series of pulses into the fiber and records the return of the naturally occurring scattered signal against time. In doing this, the distributed sensor measures at all points along the fiber. The optical fiber is made of pure glass (silica) as thin as a human hair. It consists of two parts: the inner core and the outer cladding. Cladding is a glass layer made up of lower refractive index glass to maintain guidance of light within the core. Both parts are encapsulated by a single or multiple layers of primary polymer coatings for protection and easiness of handling.

There are two main types of optical fibers according to communication application standards. These are the singlemode, intended for long haul communications, and multimode for short haul communications. Multimode fibers have a larger core (45 to 50 microns) than single mode fibers (8-10 microns), allowing more light modes to propagate. The typical diameter of an optical fiber is 125 microns that increases to 250 microns if we include the thickness of standard acrylate coating. Multimode fibers are usually used for temperature sensing, whilst singlemode fibers are mostly used for distributed acoustic sensing or strain sensing.

Although Silixa's temperature and acoustic sensors can be used with either single mode or multimode fiber, the performance of the acoustic sensor is optimized with single mode fiber. Fiber optic cables can contain many fibers, which can be either a single type or a combination of both. The cable construction depends on the installation, operation and application conditions.

iDAS technology measures the acoustic signal at all points along many kilometers of the optical fiber as if it were a string of microphones. The iDAS works by injecting a pulse of laser light into the optical fiber. As this pulse of light travels down the optical path, interactions within the fiber, which result in light reflections known as backscatter, are determined by tiny strain events within the fiber which in turn are caused by localized acoustic energy. This backscattered light travels back up the fiber towards the iDAS where it is sampled. The time synchronization of the laser pulse allows the backscatter event to be accurately mapped to a fiber distance.

Once the pulse of light has travelled to the end of the fiber and any reflections have travelled back to the interrogator the fiber can be considered to be “dark” and a subsequent laser pulse can be introduced without the risk of interference. For each laser pulse the entire fiber distance is sampled at each point along the length, typically at every 1 meter. The result is continuous acoustic sampling along the entire length of the optical fiber without cross talk and with a frequency range from milli-Hertz to over 100 kilo-Hertz and a dynamic range of over 120 dB.

DAS does not discriminate between the different spatial components of the ground movements (vertical, horizontal in-line with the cable, horizontal perpendicular to the cable), even if the sensitivity is a function of the angle of incidence as reported by Wu et al. (2017). The fiber optic is more sensitive to compressional (P) waves with low-degrees of incident angle (waves propagating in the same direction of the cable), while it is essentially blind to events that propagate perpendicular to the fiber optic. The stronger DAS response to shear (S) waves occurs when the incident angle is around 45 degrees and damps down to no recorded signal for higher and lower incident angles.

Signal to Noise Ratio (SNR) in DAS measurements is largely governed by how much light can be usefully collected from the optical fiber. The ideal fiber should have low signal loss to be able to achieve long ranges, but also high scattering to enhance the amount of reflected light. This apparent contradiction is overcome by the use of a new type of fiber (constellation), where engineering bright scatter centers are implemented along the fiber without introducing significant excess loss in the forward propagating scattered light. Using a dedicated interrogator together with the engineered fiber (Carina system), SNR is lowered down by 20 dB, equivalent to an improvement of 100 times.

2.1.2 Geode system - London test

The measurement system for the London test was comprised of a 3*24 channel Geometrics Geode system with 24 3-axial 4.5 Hz geophones (Figure 2.1.1).

The source consisted of a 5 Kg sledge hammer applied vertically on a plate and horizontally in the end of a wooden beam (Figure 2.1.2).



Figure 2.1.1. Line of 3-axial geophones for the London test



Figure 2.1.2. Wooden beam as SH source for the London test

2.1.3 DMT system - ESS site

The measurement system for the test on stabilized ground at the ESS facility consisted of a 100 channel DMT Summit X One system with 50 2-axial 4.5Hz geophones, vertical and inline horizontal (Figure 2.1.3).

The source consisted of an ESS100 Turbo accelerated weight drop applied vertically on a plate. Shots were also made with a 5 Kg sledgehammer horizontally in the end of a wooden beam (Figure 2.1.3).



Figure 2.1.3. ESS100Turbo accelerated weight drop. The Summit X One Remote Units are also visible together with two geophones next to the wheel of the weight drop.

2.2 Processing

Seismic waves are divided into body waves, compressional (P) and shear (S) waves, and surface waves, like the Rayleigh, Lamb or Scholte waves (e.g. Telford et. al 1990). In the soil stabilization application work presented in this report we focus on analysis of surface waves, as a base for mapping S-wave velocities, but also look generally at the wavefield and how data from geophones compare with data from fiber by looking at e.g. direct or refracted P-waves and S-waves.

2.2.1 Analysis: Time-Space (TX) and Frequency-Wavenumber (FK) domain

In the present report, acoustic data are in many places represented as seismogram images with a colored pixel for each sample. The seismograms display the amplitude of the recorded signal in time (T) and space (X). They are also named TX plots.

Fig. 2.2.1 shows the colorbar used for almost all the seismograms plotted in the report. The colorbar is scaled on the absolute maximum amplitude of the recorded waves for each dataset. A direct comparison of the amplitudes recorded by the different seismic techniques is not possible as the acoustic signals are acquired with completely different sensors.

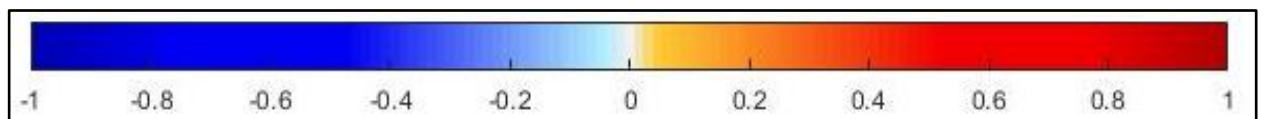


Figure 2.2.1. Colorbar used for the seismograms (TX) displayed in the present report. Energy is normalized on the absolute maximum value.

The aim of the project is to investigate capabilities and limitations of the fiber optic as an acoustic sensor for engineering applications. For achieving this goal, it is important to analyze the frequency content of the recorded signal, both in time and space. A tool often used in seismic is what is commonly called the FK plot, where a double Fourier transform is applied: time (T) is transformed to frequency (F) and space (X) is transformed to wavenumber (K). This representation displays the distribution of energy magnitude according to the frequency content.

This tool facilitates the analysis of the frequency content of the acoustic data and permits a better comparison between fiber optic and traditional seismic techniques. The tool enhances if a technique is able to acquire the same frequency range of the other methodology. Moreover, FK plots reveal also the role of the different resolutions in the acoustic soundings.

The FK plots highlight the frequency content of surface waves, since they are the most energetic. Less energetic seismic events as refracted and reflected waves are characterized by lower magnitude, so they are not easily detectable in these kinds of analysis. There is also a higher interest in surface waves analysis for investigating stabilized soil, as they might provide information about relevant physical parameters related to the stiffness of the material (i.e. S-wave velocities).

Fig. 2.2.2 shows the colorbar used for all the FK plots in the report. The colorbar is scaled on the maximum magnitude of the energy distribution of each dataset.

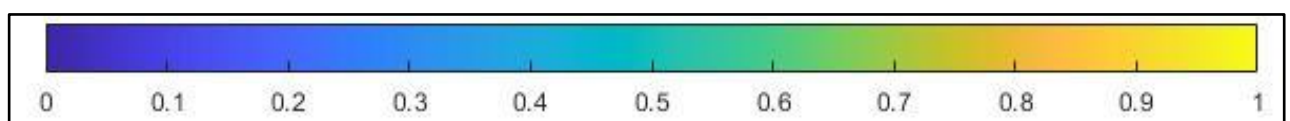


Figure 2.2.2. Colorbar used in the FK (double spectral) plots displayed in the present report. Energy is normalized to the maximum magnitude.

Another set of plots analyzed in the report is obtained calculating the spectra (F) via Fourier transform only along the time axis, while keeping the space (X) in the second data dimension. This kind of representation, here named FX, gives a clear picture on how the frequency content may vary along the acquired profile. The same colorbar as FK plots is adopted (Fig. 2.2.2).

3. FIELDWORK

For achieving the goals of the project several tests have been performed. We also changed the initial plan during the development of the project, for adapting to new needs and trying to obtain the most useful information for the present feasibility-test project.

3.1 Pillar Gothenburg

A preliminary test for installing a fiber optic cable in a pillar, constructed via soil-binder mixing in situ by NCC, has been performed by Hydroresearch AB. The site was located at the construction site Centralen in Gothenburg.

Unfortunately, we could not perform acoustic measurements along this pillar, as the installation was not anymore available when the equipment was in Sweden for the other tests. Moreover, it would have been logistically difficult to compare DAS acquisitions with other standard methods. The main problem being the collocation of sensors that is a key aspect to validate the results from the fiber optic survey. For this reason, the site was downgraded to a lower priority. Nevertheless, after the knowledge acquired from the other test sites (where we could compare fiber optics and traditional acoustic sensors), the possibility of installing fiber optics in soil-binder mixing pillars could be an interesting opportunity for further experiments and for establishing a new methodology able to assess the integrity of such underground structures.

3.2 London test

The first field test has been performed on 5th and 6th December 2018 at Silixa test facility in Elstree, Hertfordshire (UK), where several fiber optic cables are buried in natural soil at a depth of about 30 cm. The experiment has been conducted measuring along the fiber optic cables using two different Silixa acoustic instruments: iDAS v3 and iDAS v2 (for the specifications of the acquisition parameters see Tab. 3.2.1).

Several lines with 3-component 4.5 Hz geophones were placed on the topographic surface, exactly on top of the buried fibers. The aim was recording with a standard seismometer (Geode, Geometrics) that has been used for the comparison with fiber optic data.

The location of the test has been decided for several reasons:

- the convenience of having already installed fiber optic cables
- the site has been extensively used by Silixa, for testing their equipment
- the availability of experts from Silixa
- the possibility of testing 2 different instruments for interrogating the fiber optics.

This field test was essential to get familiar with the new type of acoustic data and to define their capabilities and limitations compared to the standard geophone seismometers.

The source was a sledge hammer of 5 kg. We acquired data moving the source in several positions along the profile and also with a lateral offset from the linear location of the sensors. S-waves have additionally been generated shouting laterally on a large oak beam (of the type of railway beams).

Parameters	iDAS v3 (Silixa)	iDAS v2 (Silixa)	Geode (Geometrix ltd)
<i>spatial resolution [m]</i>	2	10	punctual
<i>spatial sampling [m]</i>	0.255	1.021	3, 1 and 0.5
<i>time sampling interval [s]</i>	$2e^{-4}$	$2e^{-4}$	$2e^{-5}$
<i>time window [s]</i>	1	1	from 0.7 to 1.36

Table 3.2.1. Acquisition parameters for the different acoustic systems used in the London test.

3.3 ESS site

The site is located in the municipality of Lund (Sweden), where the new European Spallation Source infrastructure is under construction. Thanks to Skanska Sverige AB, we had the opportunity of performing surveys on top of a slab of stabilized soil, where the comparison between fiber optics and traditional sensors is logistically facilitated, unlikely along the pillar of the Gothenburg site.

The soil has been stabilized mixing layers of natural soil material (clay till deposit) and layers of binder (quicklime). The area is about 30x20 m and the thickness of the treated soil is around 1.5 m (Fig. 3.3.1), even if the compaction of the soil during the stabilization process could affect a deeper portion of the ground.

A profile with a maximum length of 90 m has been designed in the area with the aim of investigating both the stabilized and the natural soil (Fig. 3.3.3). Along this profile a 30 cm deep trench has been excavated for installing the fiber optic cable (Silixa engineered fiber) within the ground (Fig. 3.3.2). This aspect is essential to ensure a good coupling between the cable and the surrounding material: a key point for the transmission of acoustic energy from the ground to the cable. The fiber optic cable has been placed in the ditch on a 2-3 cm bed of medium grain sand to avoid damages along the fiber. Damages could happen if the cable is in contact with large cobbles that are present in the till deposit. The trench has been backfilled with an analog thin

layer of sand and on top of that with the soil previously excavated. The backfilled ditch has been compacted by the wheels of a heavy machine.

The geophones have been placed on top of the installed fiber optic cable and they are well collocated as it evinces from the differential GNSS coordinates acquired along the fiber optic cable and at the geophones locations (Fig. 3.3.4 A). Looking at the elevation of the sensors (Fig. 3.3.4 B), we can assure that the position of the cable in the ground is about 30 cm from surface along the entire profile.

Along the profile we acquired 3 layouts of geophones with different spacing between the receivers, while the acquisition of fiber optic data always involved the entire profile with fixed parameters. Table 3.3 summarizes the parameters of the acquisitions. For the standard seismic measurements we used the SUMMIT X ONE (DMT GmbH & Co. KG) equipment with vertical and horizontal 4.5 Hz receivers. Figure 3.3.5 shows an example from Layout 3, where vertical and horizontal geophones are located on top soil with a spacing of 0.5 m.

As source of acoustic waves we used an accelerating drop (see section 2.1.3) to be able to transmit enough energy in the ground. This kind of source was necessary to contrast the environmental noise, which was mainly due to active construction works in adjacent areas and the heavy traffic along Highway E22 (visible in the north-west corner of Fig. 3.3.1). For the specifications of the acquisition parameters see Tab. 3.3.1.

Parameters	Fiber optic (Carina)	Layout 1 (geophones)	Layout 2 (geophones)	Layout 3 (geophones)
<i>spatial resolution [m]</i>	2	punctual	punctual	punctual
<i>spatial sampling [m]</i>	0.255	2	2	0.5
<i>time sampling interval [s]</i>	$2e^{-5}$	$1.25e^{-4}$	$1.25e^{-4}$	$1.25e^{-4}$
<i>time window [s]</i>	1.2	1.2	1.2	1.2
<i>local coordinates along the profile [m]</i>	0-90	0-88	1-89	5-24

Table 3.3.1 Acquisition parameters for the different acoustic systems used at the ESS test.

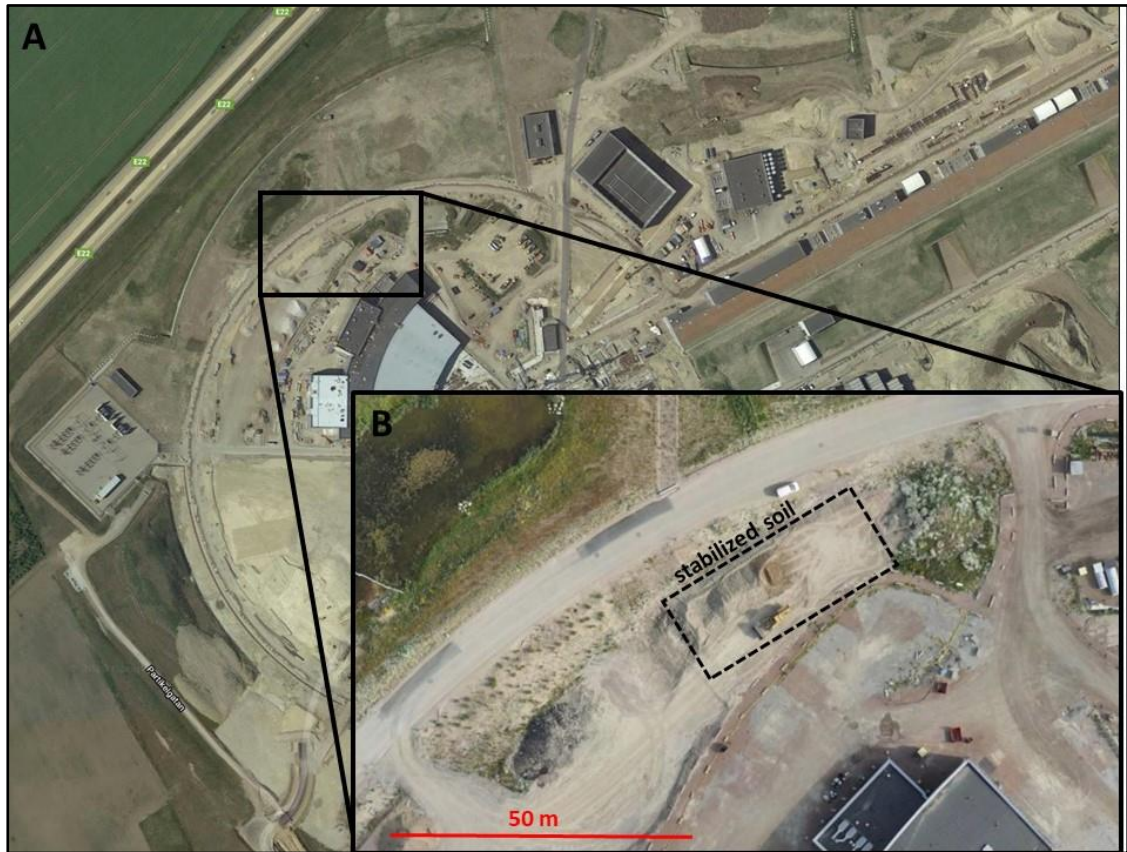


Figure 3.3.1. A) Google Map image of the construction area. B) High detailed orthophoto of the area during the construction of the stabilized slab (courtesy of Skanska ESS Construction).



Figure 3.3.2. Pictures of the installation of the fiber optic cable in the ground: left, digging of the trench; middle, cable on top of sand layer; right, backfilling of the ditch with sand and excavated material.

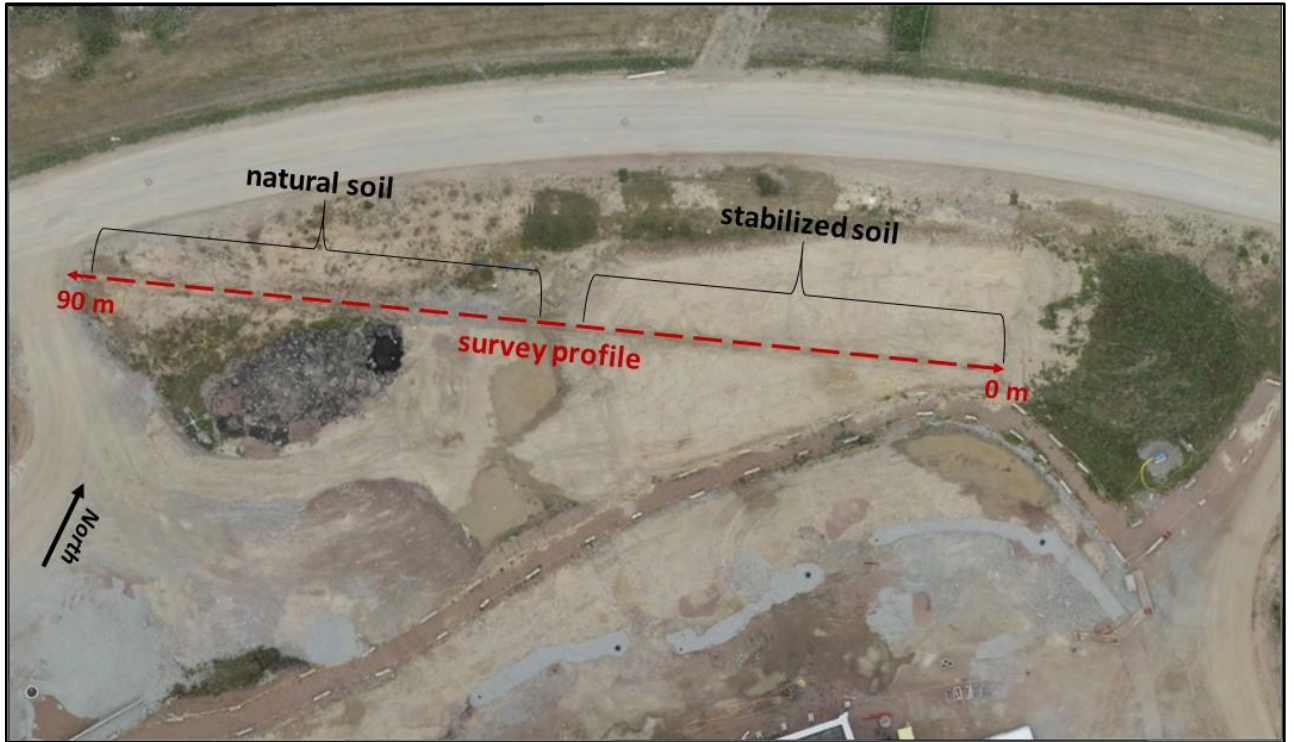


Figure 3.3.3. Location of the survey profile with the local coordinates used for the different acquired layouts. The orthophoto (courtesy of Skanska ESS Construction) has been acquired closely after the geophysical survey; the mark of the trench on the top soil is still visible.

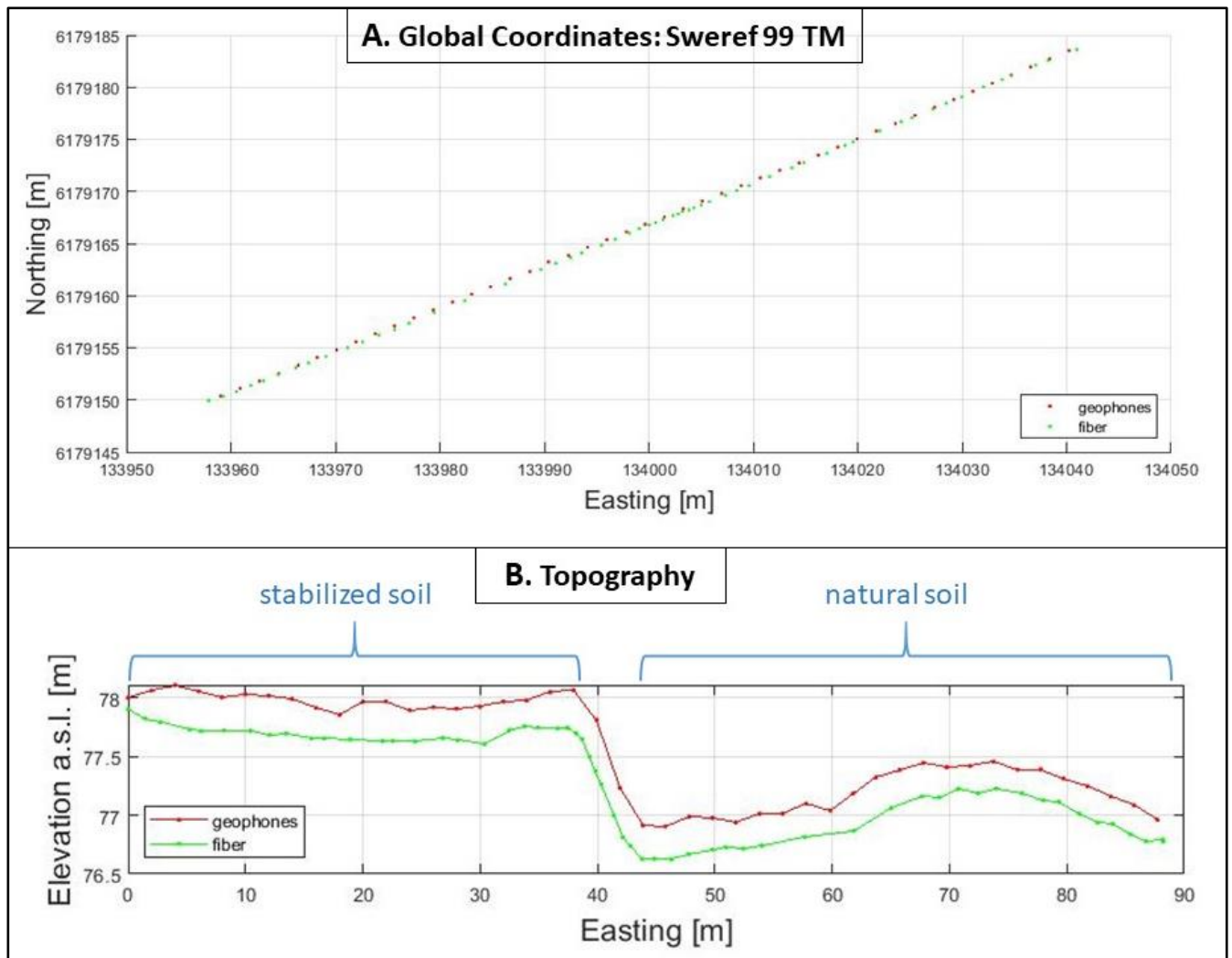


Figure 3.3.4. Global coordinates of the location of the fiber optic cable (green dot/line) and the geophones (red dots/line). Plot A shows the planar Sweref 99 TM coordinates, while plot B shows the elevation of the sensors along the profile.



Figure 3.3.5. Example of geophones layout: Layout 3 with 0.5 m spacing, 4.5 Hz geophones. Yellow receivers are the vertical component geophones, while the red ones are the horizontal (in-line) component geophones.

3.4 Pile experiment

The third experiment has been designed for testing capabilities and limitations of DAS as an acoustic sensor for civil engineering applications. We performed measurements on a reinforced precast concrete pile that is commonly used for the support of buildings and other structures in Sweden. The experiment took place at Peab Grundläggning AB (Tollarp, Sweden).

A fiber optic (Silixa engineered fiber) has been inserted in a concrete pile of dimensions 14x0.4x0.4 m (Figure 3.4.1). The cable has been firmly attached at the metal armor, before the pouring of concrete (Figure 3.4.2). The fiber optic is placed on one side of the pile, along the higher dimension, then it turns back along the bottom side for a total of about 28 m of cable installed inside the pile (see also Figure 4.3.2). This procedure ensured an excellent coupling of the cable with the surrounding material, increasing the sensitivity. The test has been performed comparing the DAS soundings from the Carina system (Silixa) with an accelerometer. Parameters of the two acquisition systems are summarized in Tab. 3.4. The accelerometer measurements are a standard for testing the integrity of those kinds of piles, when placed into the ground (low strain pile integrity test).

The source of acoustic waves was a small hammer, manually operated, as it is common for testing piles with accelerometer receivers (Figure 3.4.3). The accelerometer was located on the smaller side of the pile, close to the insertion of the fiber optic cable. The accelerometer provides a single point measure, while the fiber optic produces information along the entire length of the cable. For the specifications of the acquisition parameters see Tab. 3.4.1.

Parameters	Carina (Silixa)	Accelerometer
<i>spatial resolution [m]</i>	2	punctual
<i>spatial sampling [m]</i>	0.255	-
<i>time sampling interval [s]</i>	$1e^{-5}$	$1e^{-5}$
<i>time window [s]</i>	about 1	1

Table 3.4.1 Acquisition parameters for the different acoustic systems used in the Pile test.



Figure 3.4.1. The pile used for the experiment. The fiber optic cables that come out from concrete are visible on the top portion of the pile.

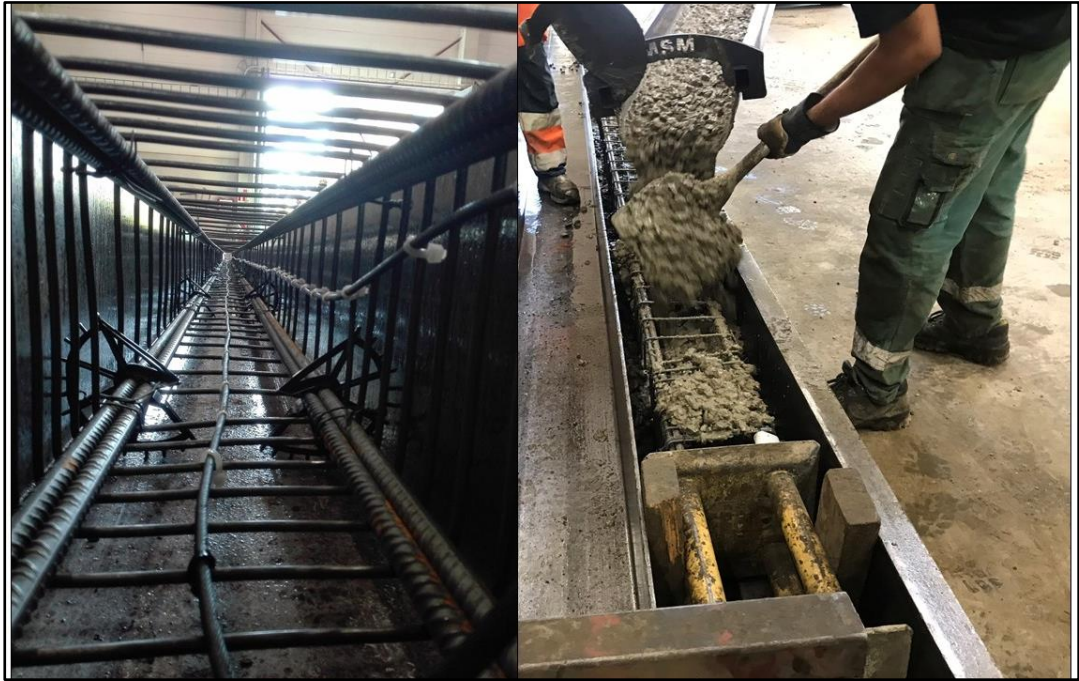


Figure 3.4.2. Installation of the fiber optic cable inside the concrete pile. The left picture reveals how the cable has been firmly anchored on the metal armor along a lateral and the bottom sides of the pile. The right picture shows the operation of pouring cement.



Figure 3.4.3. Nils Rydén (Peab AB and Lund University) acquires measurements with an accelerometer placed on the smaller side of the pile.

4. RESULTS AND DISCUSSION

4.1 London test

The knowledge acquired from this preliminary study has been essential for planning further tests. This experience has been crucial to adapt and better design further experiments. Looking at the capabilities and limitations of the fiber optic interrogators compared to the traditional geophones array, we decided to limit the following experiments at the Carina system together with the engineered fiber, as the higher resolution of this set-up is an essential requirement for the civil engineering applications that are the aim of the project.

Results from this test are not presented here, since they do not add more information than the experiments that followed and that are presented in chapter 4.2. Moreover, the data quality of the acquisitions in the London test is inferior to successive surveys on other sites, partially due to the source of seismic waves utilized and partially derived by the geology of the area. The site furthermore does not present those characteristics requested by the projects: an area of artificially stabilized soil and underwater conditions.

4.2 ESS site experiment

The ESS site gives the opportunity to compare traditional and DAS sensors for an engineering application concerning soil stabilization. It was essential to measure on an area where a stabilization procedure was completed, since the acoustic wave velocities are different in different media and predictably higher in stiffer stabilized materials. The correct estimation of acoustic wave velocities in their higher limit is also depending on the resolution of the technique. This is therefore a key point to test the method in such conditions.

The results here presented refer only to acquisition where the source was placed external to the profile (external shots), even if we acquired data shooting also along the line between the geophones. Data recorded with external shots have a higher quality and better show the entire frequency and wavelength content.

Both Layout 1 and 2, with a 2 m inter-geophone spacing (Tab. 3.3.1), cover partially the area of stabilized soil and partially the natural soil (Fig. 3.3.2). Layout 2 is analogue to Layout 1, the only difference is that the entire line of geophones has been moved 1 m along the profile. This gives the possibility to combine the acquisitions of both layouts and finally obtain a profile with 1 m resolution. The integration of Layout 1 and 2 has been done stacking seismograms with the same source location, after a careful processing and adjusting of time zero. For comparison also the fiber optic data has been stacked.

Fig. 4.2.1 shows an example of raw seismograms for Layout 1. The green arrows indicate the limit between the left stabilized soil and the right traces on the natural soil. The transition between the two areas is affected also by a change in topography, coinciding with a slope (Fig. 3.3.4 B). A clear change in wave propagation is visible in this portion of the seismograms.

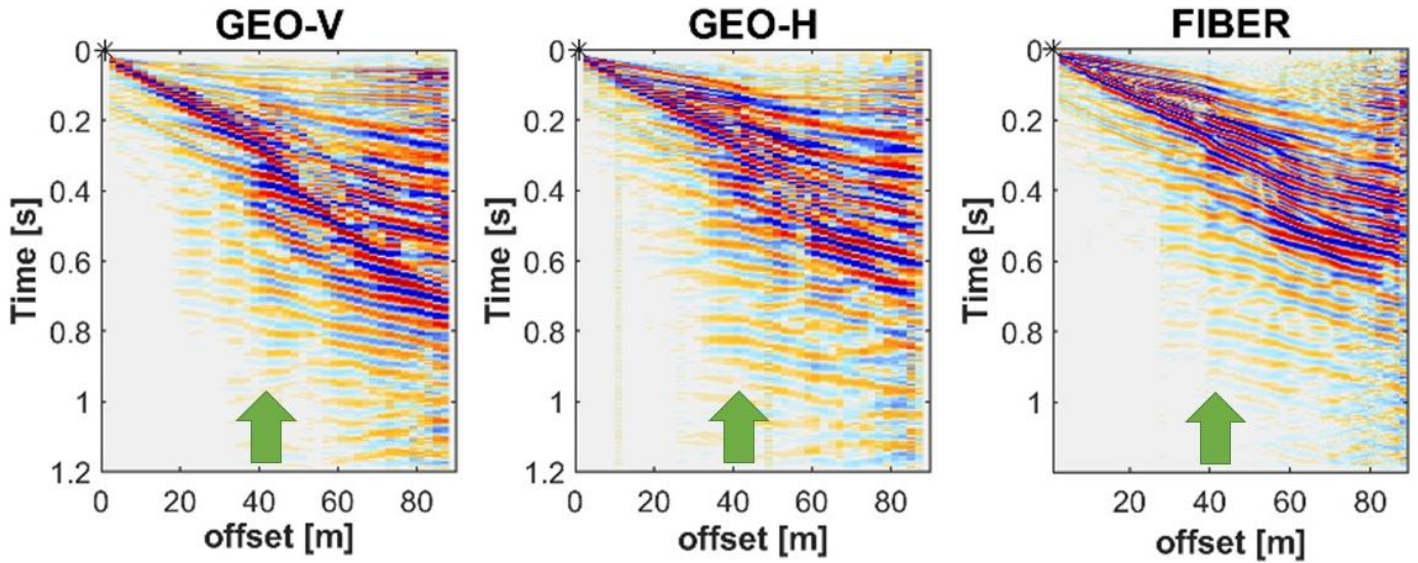


Figure 4.2.1. Example of seismograms from Layout 1 survey: left, vertical geophones (GEO-V); middle, horizontal in-line geophones (GEO-H); right, fiber optic sensors (FIBER). The green arrow indicates the transition zone between stabilized soil (left) and natural soil (right). The black asterisk is the location of the source.

The seismograms of Fig. 4.2.1 show a comparable behavior; in particular, the DAS and the horizontal geophone (GEO-H) data present a high similarity. This higher similarity between DAS and GEO-H seismograms is a common characteristic of all the datasets acquired at the site. This is mainly due to a similar contrast in relative amplitudes of different seismic events. The seismograms that display the data of the vertical geophones (GEO-V) show high energetic surface waves compared to direct arrivals. A less strong contrast is visible with the other two acquired sensors. This means that fiber optic sensors are less sensitive to vertical displacements of the ground and more sensible to horizontal movements along the cable. It is the proof of a characteristic that was expected. DAS measures the stretch of fiber, so is more sensible to movements that occur along the fiber optic cable and less sensible to acoustic waves that hit the fiber optic cable perpendicularly.

A relevant aspect that has been highlighted by the present study is the combined effect of the spatial resolution and the spatial sampling of the fiber optic data. We acquired a seismic trace every 0.255 m along the fiber that is the difference in the signal recorded at 2 m intervals along the cable. One outcome of this integration is the stepwise appearance of the fiber optic data, as it is particularly evident in Fig. 4.2.2, which shows the seismograms of Layout 3. The horizontal geophones (left plot) have a punctual resolution and a spatial sampling of 0.5 m. Even if the spatial frequency is lower than the fiber optic data, the seismogram looks smoother and the seismic events have a linear appearance. The DAS seismogram (right plot) shows a stepwise behavior that is more pronounced in some portion of the profile, reaching a maximum of 8 traces (2 m) that display a similar pattern. This is a consequence of the discrepancy between the spatial

resolution and the spatial sampling of the DAS system. Along the 2 m resolution segment some points can record a stronger signal that is dominant and commonly present in few traces. The stronger signal in some point can be the consequence of a local greater coupling of the cable with the surrounding soil. This localized and more intense stretching of the fiber masks the weaker signals from the other portions of the 2 m segment.

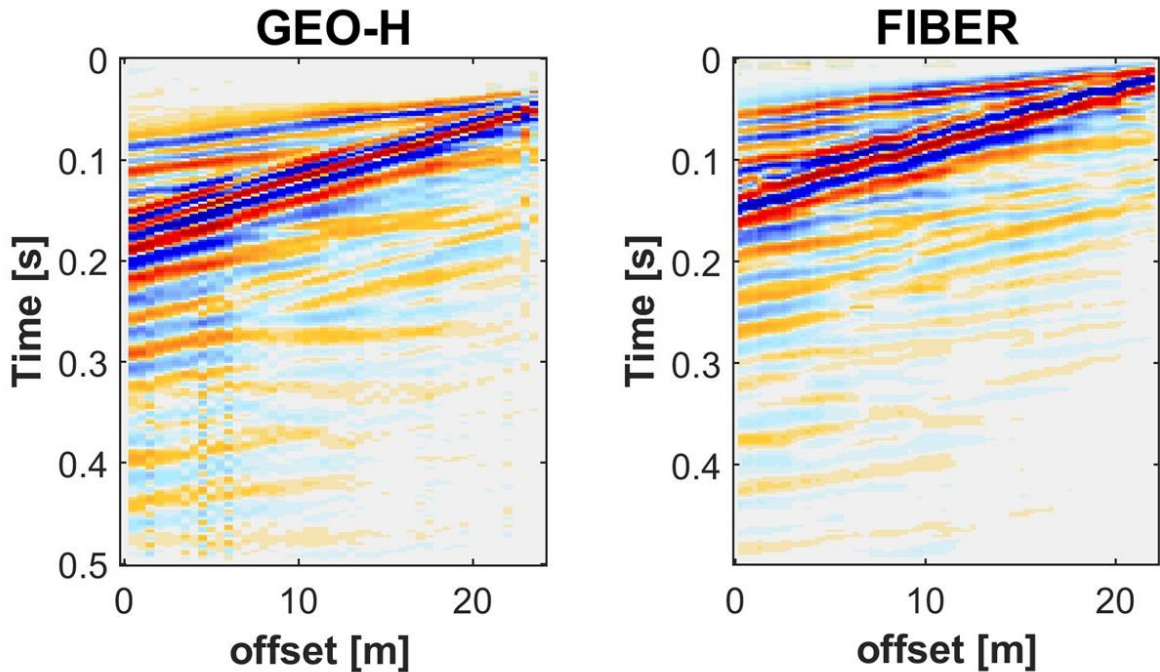


Figure 4.2.2. Example of seismograms from Layout 3: left, horizontal in-line geophones (GEO-H); right, fiber optic sensors (FIBER). It is visible the effect of the 2 m resolution in the fiber optic data.

To further investigate capabilities and limitations of the techniques, it is necessary to analyze the frequency content of the data. The profile has been divided in two portions: the area of the stabilized soil from 0 to 37 m and the area of the natural soil from 45 to 90 m, avoiding the central part characterized by the transition zone and the topographic slope. To display the frequency content of the acquired datasets, we transformed and plotted the data in the FK-domain (see chapter 2.2.3).

Figures 4.2.3 and 4.2.4 show the data of an external shot of Layout 1 (2 m spacing between geophones), for the stabilized soil and for the natural soil respectively. It is evident that frequency content is analogous between the DAS and the geophone data; in particular, the acquisition with fiber optics presents higher similarities with the horizontal in-line component of the geophones, both in TX and FK plots.

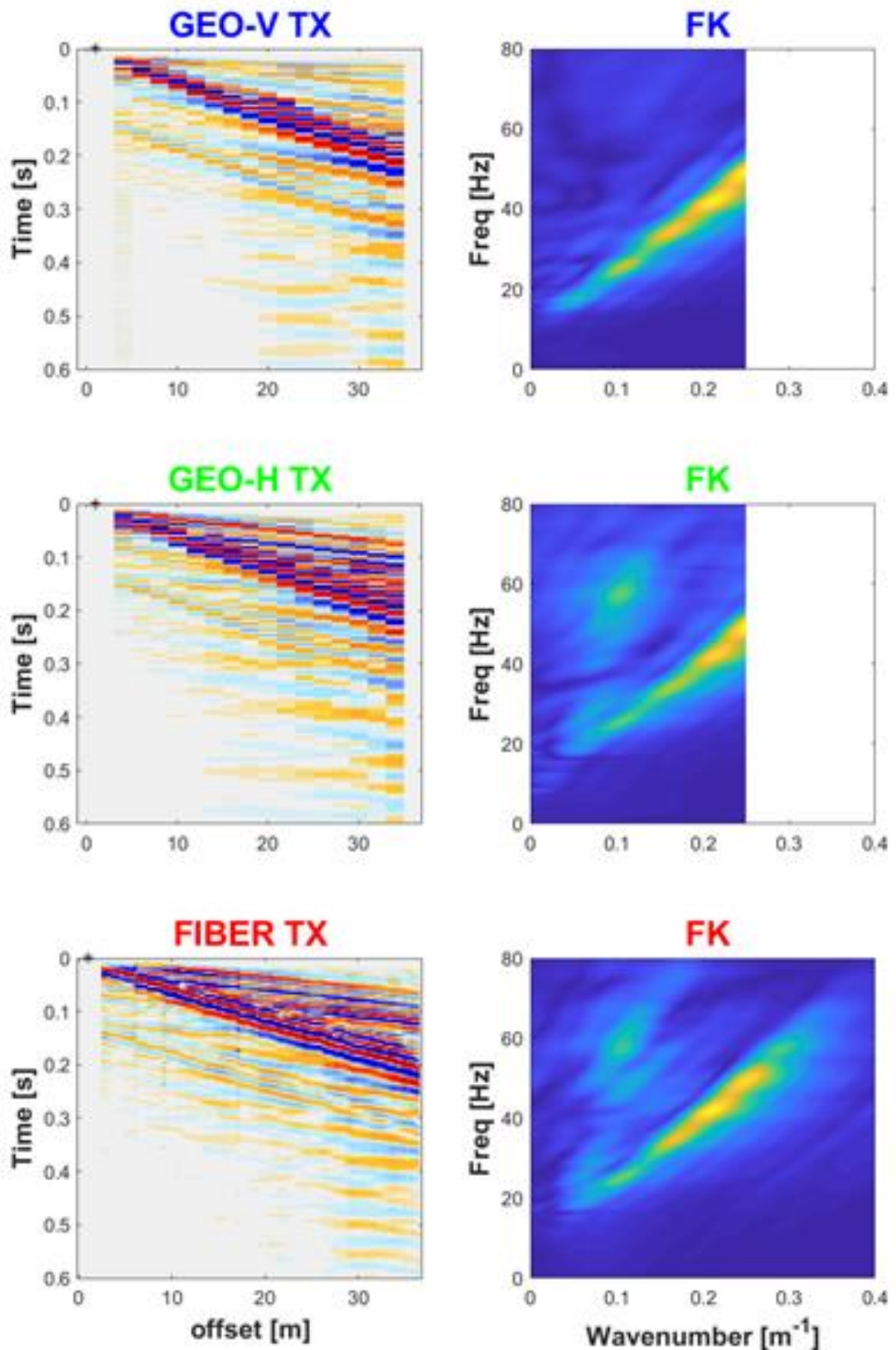


Figure 4.2.3. Example of Layout 1 (2 m geophone spacing) in the portion of stabilized soil. In the left column, the seismograms of (from top to bottom): vertical geophones (GEO-V), horizontal in-line geophones (GEO-H) and fiber optic sensors (FIBER). In the right column, the corresponding frequency content plotted as a double Fourier transform (FK).

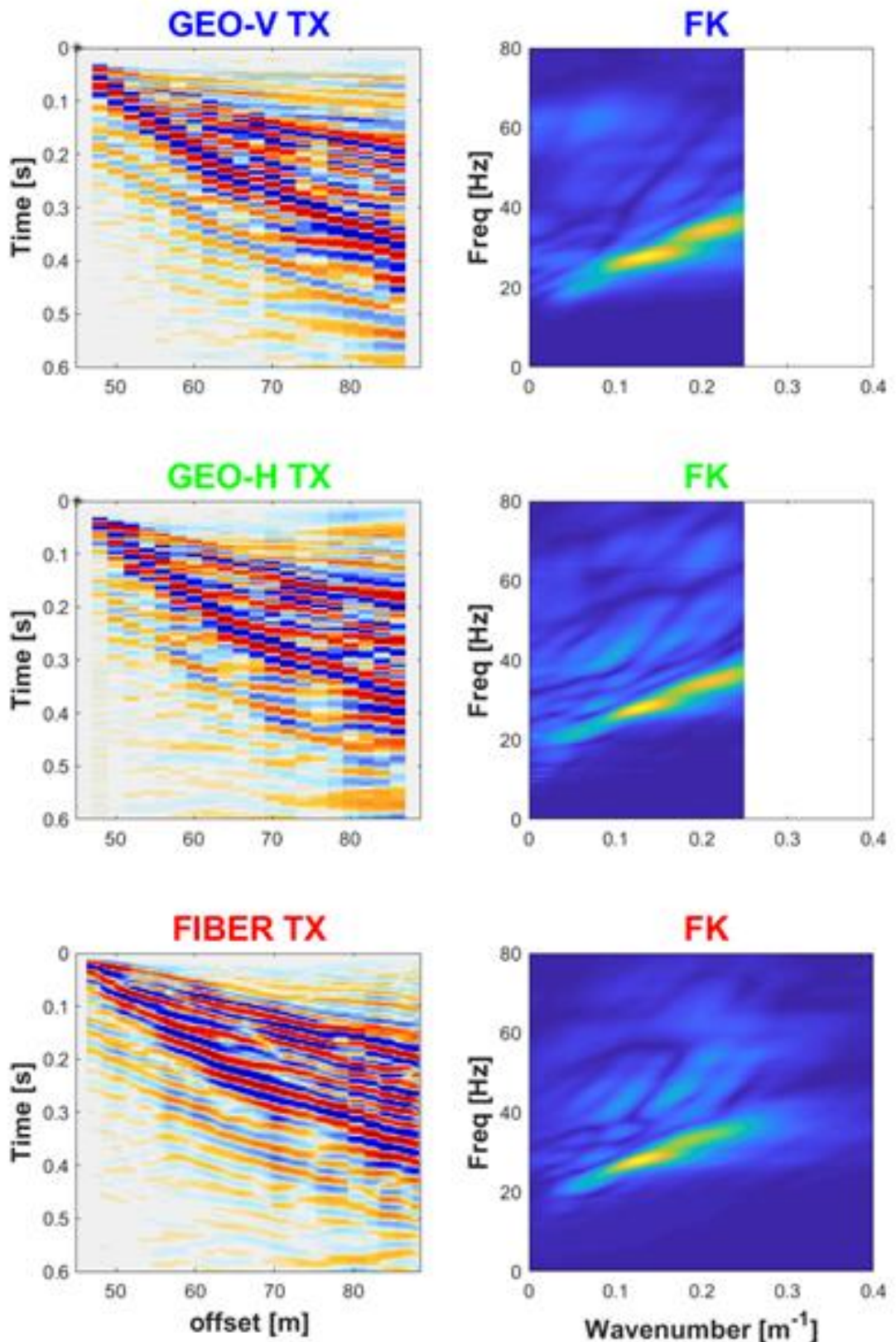


Figure 4.2.4. Example of Layout 1 (2 m geophone spacing) in the portion of natural soil. In the left column, the seismograms of (from top to bottom): vertical geophones (GEO-V), horizontal in-line geophones (GEO-H) and fiber optic sensors (FIBER). In the right column, the corresponding frequency content plotted as a double Fourier transform (FK).

This analysis confirms that fiber optic sensors record an acoustic signal that is totally comparable with traditional surveys via geophones. It is evident both in the seismograms and in the FK plots, where the energy distribution shows the same pattern.

Fig. 4.2.3 (stabilized soil) is in general characterized by higher velocities of acoustic waves compared to Fig. 4.2.4 (natural soil); this is evident from the different slopes of seismic events, both in TX and FK plots. Both technologies are able to detect variations in the wave propagation, caused by contrasting material properties.

The high similarity in Fig. 4.2.3 and Fig. 4.2.4 is also a consequence of the same resolution of both techniques: 2 m (Tab. 3.3.1). If we analyze instead Fig. 4.2.5 (stabilized soil), where the data from the geophone Layout 1 and 2 have been integrated to obtain a final resolution of 1 m, some differences are present. The most evident discrepancy is the distribution of the higher energetic event, which is related to surface waves. DAS data are not able to reveal the signal at higher frequencies and higher wavenumbers, i.e. this is the signal that comes from shorter wavelengths. This outcome may be the consequence of the 2 m resolution of the fiber optic sounding, even if the spatial sampling comes with a higher frequency (0.25 m; see Tab. 3.3.1).

The difference in the energy distribution inferable from Fig. 4.2.6 (natural soil) is less pronounced, because in this case the soil is characterized by different material properties, and especially by slower acoustic wave velocities that are characterized by lower frequencies and lower wavenumbers. In particular, the data from the horizontal geophones are more similar to DAS data, where larger wavelengths (smaller wavenumbers) are not present. In Fig. 4.2.5 and Fig. 4.2.6 the maximum wavenumber present in the fiber optic signal is around 0.25 m^{-1} , which means that we are able to detect wavelengths with an inferior limit of about 4 m: exactly the double of the resolution (2 m). So the resolution is governing the spectra content of the recorded signal, in spite of the higher spatial sampling.

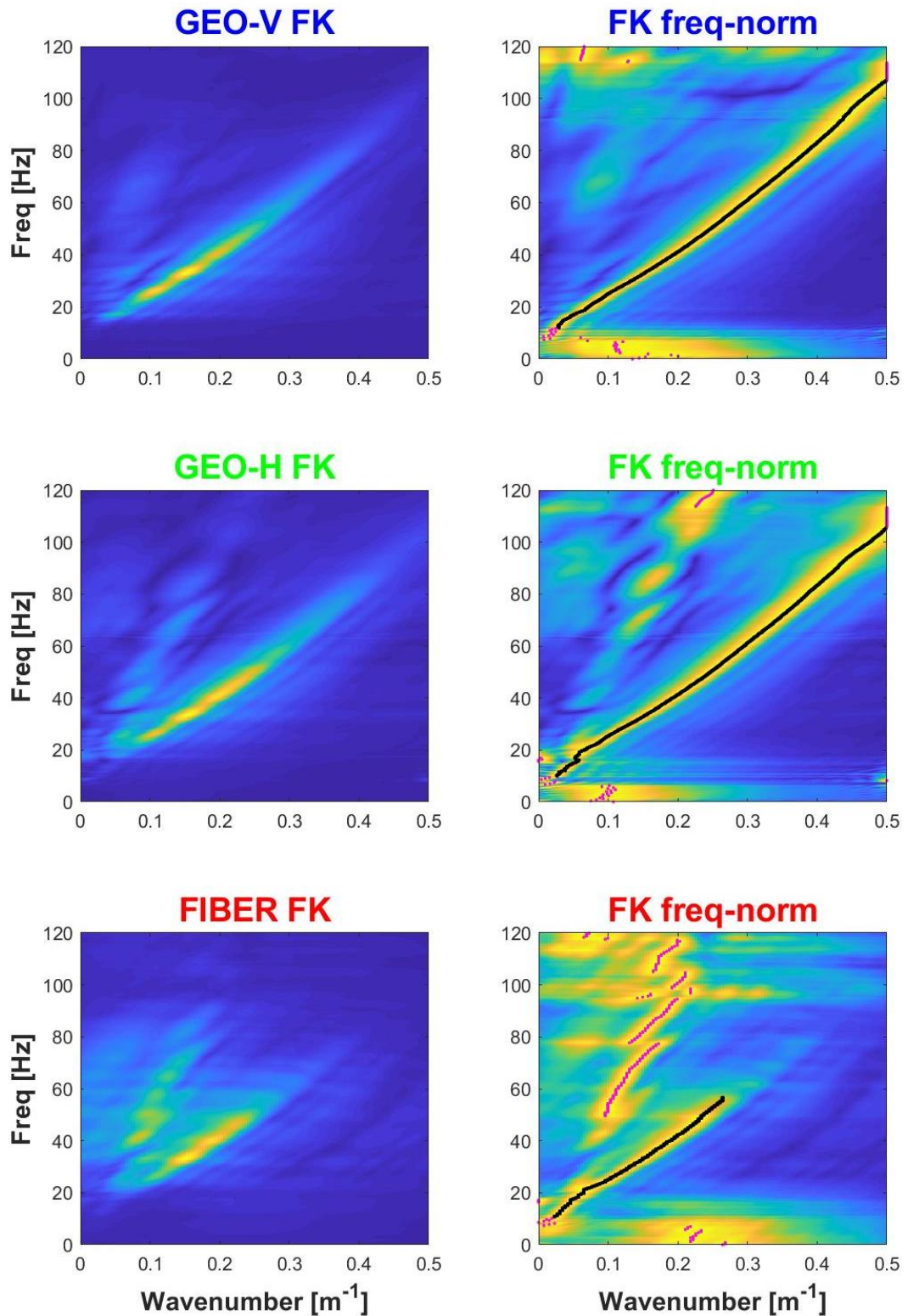


Figure 4.2.5. Example of FK plots for the combined Layout 1 and 2 datasets (1 m geophone spacing) in the portion of stabilized soil. In the left column, the FK plots of (from top to bottom): vertical geophones (GEO-V), horizontal in-line geophones (GEO-H) and fiber optic sensors (FIBER). In the right column, the same plots where the amplitude values have been normalized for each frequency. The maxima amplitudes for each frequency are plotted as magenta and black dots. Black dots highlight the fundamental mode of Rayleigh waves.

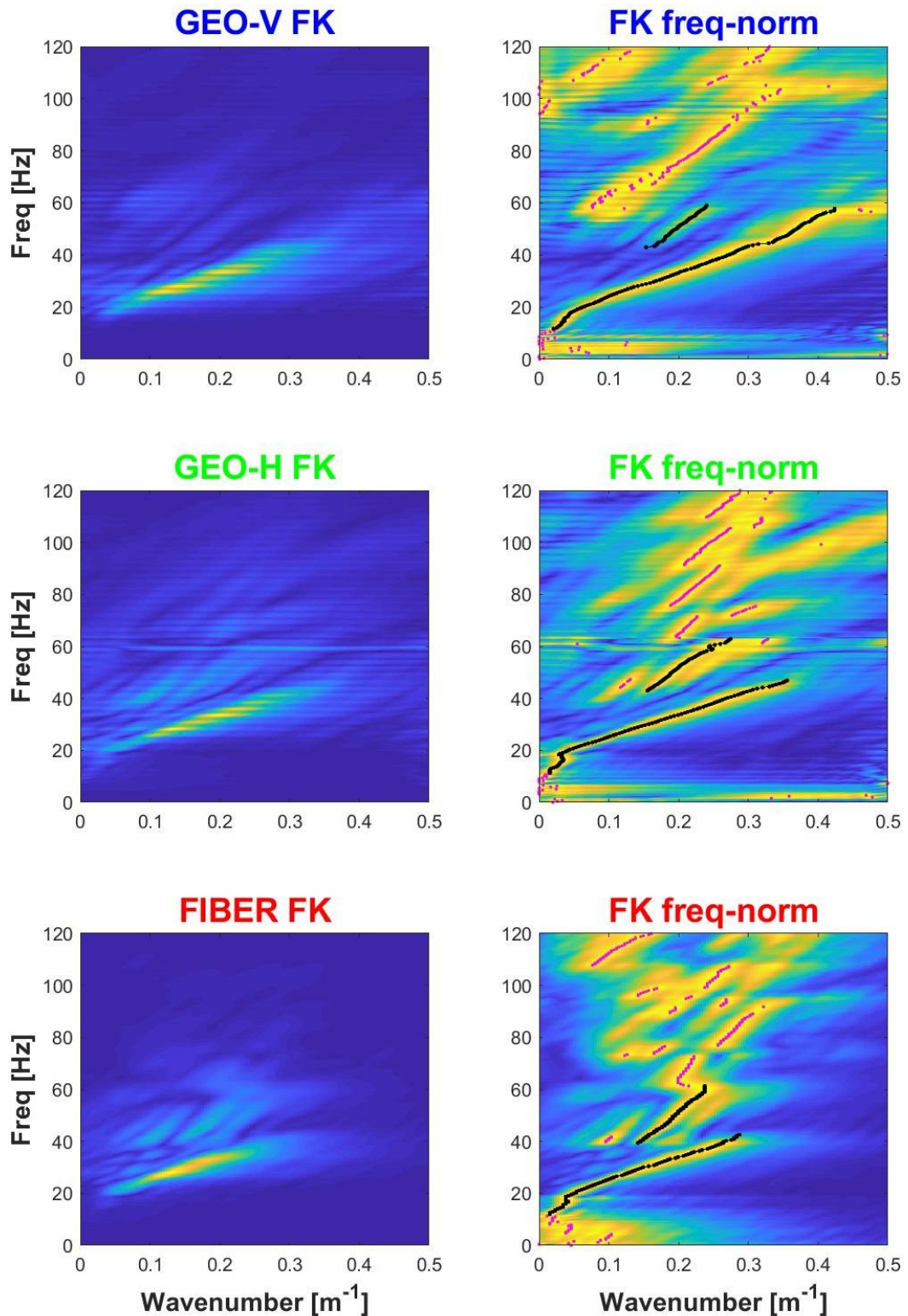


Figure 4.2.6. Example of FK plots for the combined Layout 1 and 2 datasets (1 m geophone spacing) in the portion of natural soil. In the left column, the FK plots of (from top to bottom): vertical geophones (GEO-V), horizontal in-line geophones (GEO-H) and fiber optic sensors (FIBER). In the right column, the same plots where the amplitude values have been normalized for each frequency. The maxima amplitudes for each frequency are plotted as magenta and black dots. Black dots highlight the fundamental mode of Rayleigh waves.

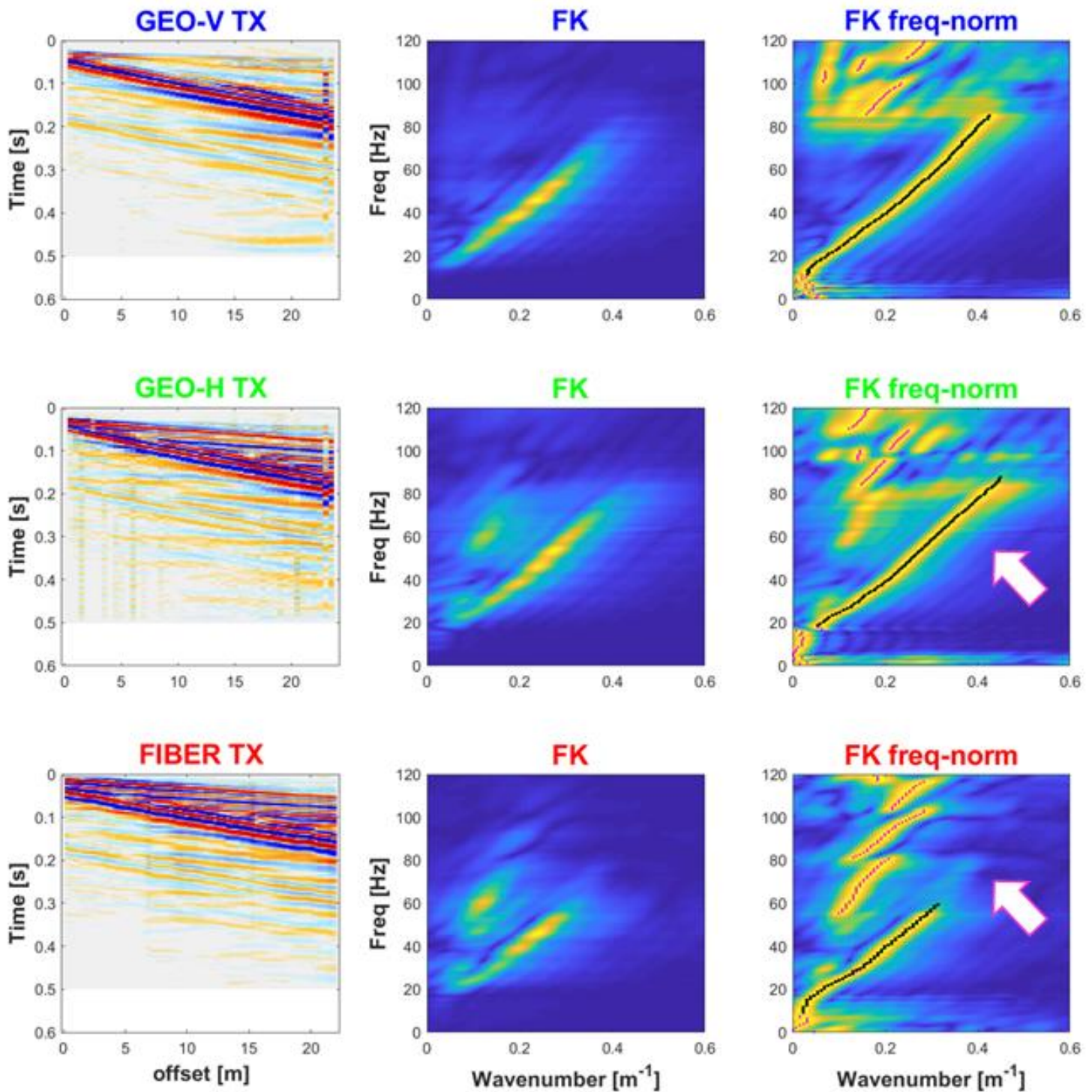


Figure 4.2.7. Example of Layout 3 (0.5 m geophone spacing) in the portion of stabilized soil. In the left column, the seismograms of (from top to bottom): vertical geophones (GEO-V), horizontal in-line geophones (GEO-H) and fiber optic sensors (FIBER). In the middle column, the corresponding frequency content plotted as a double Fourier transform (FK). In the right column, the same FK plots with the energy content normalized for each frequency. The maxima amplitudes for each frequency are plotted as magenta and black dots. Black dots highlight the fundamental mode of Rayleigh waves.

The same resolution issue is visible comparing the fiber optic spectra with the shorter spatial sampling of Layout 3 (0.5 m between geophones). Fig. 4.2.7 displays the seismograms and the FK-spectra for a shot external to Layout 3. White-magenta arrows highlight the dissimilarities in the energy distribution of the spectra. We can recognize similar characteristics of the signal as in the previous tests. This verifies the validity of our considerations. It is worth mentioning that even if we have a higher resolution in Layout 3, capable of detecting acoustic waves with 1 m of wavelength, the energy is distributed within a min of 2 m as the shortest wavelength (corresponding to 0.5 m^{-1} as wavenumber). This is a consequence of the specific material properties of the stabilized soil that place a limit in seismic wave velocities.

The FK spectra qualitatively look similar, especially between horizontal in-line geophones and fiber optic sensors, as we discussed above. They have an analogue energy distribution among the different modes of propagation. For a clearer and exhaustive comparison, the maxima amplitudes of these spectra of the three different datasets (vertical geophones, horizontal in-line geophones and fiber optic) are plotted in a single figure (Fig. 4.2.8). It is evident that the different sensors record exactly the same modes of propagation within a small variance due to inevitable environmental noise.

The fundamental mode of Rayleigh waves has been extracted for each FK spectrum, as it is displayed in the right column of Figures 4.2.7, 4.2.5 and 4.2.6 by the black dots. An inversion is conducted to extract a vertical one-dimensional profile of shear wave velocities (V_s) through the inversion algorithm presented in Vignoli et al. (2021). Fig. 4.2.9 shows the inversion results of the dispersion curves derived from the portions of stabilized and natural soil. Two V_s vertical profiles (Fig. 4.2.9 A) are obtained from the portion of stabilized soil inverting dispersion curves of Layout 3 (0.5 m spacing), light blue dashed line, and the combination of Layout 1 and 2 (1 m spacing), dark blue solid line). The distribution of V_s is almost identical especially in the shallower 8 m, where a low velocity layer ($V_s < 250 \text{ m/s}$) is identified between 0 and 3 m below the topographic surface. The inversion of seismic data from the portion of natural soil estimate a V_s vertical profile that is similar in shape to the previous profiles, but it is characterized by lower shear-wave velocities in the shallower 3 m; please note that this profile starts at a depth of 0.75 m to compensate the average difference in elevation between the two portions of the profile (see Fig. 3.3.4 B). The stabilization process has been effective, increasing V_s of about 100 m/s.

Dispersion curves obtained from DAS and from horizontal geophones have not been inverted, since the dispersion curves show an identical pattern for all the datasets (see Fig. 4.2.8).

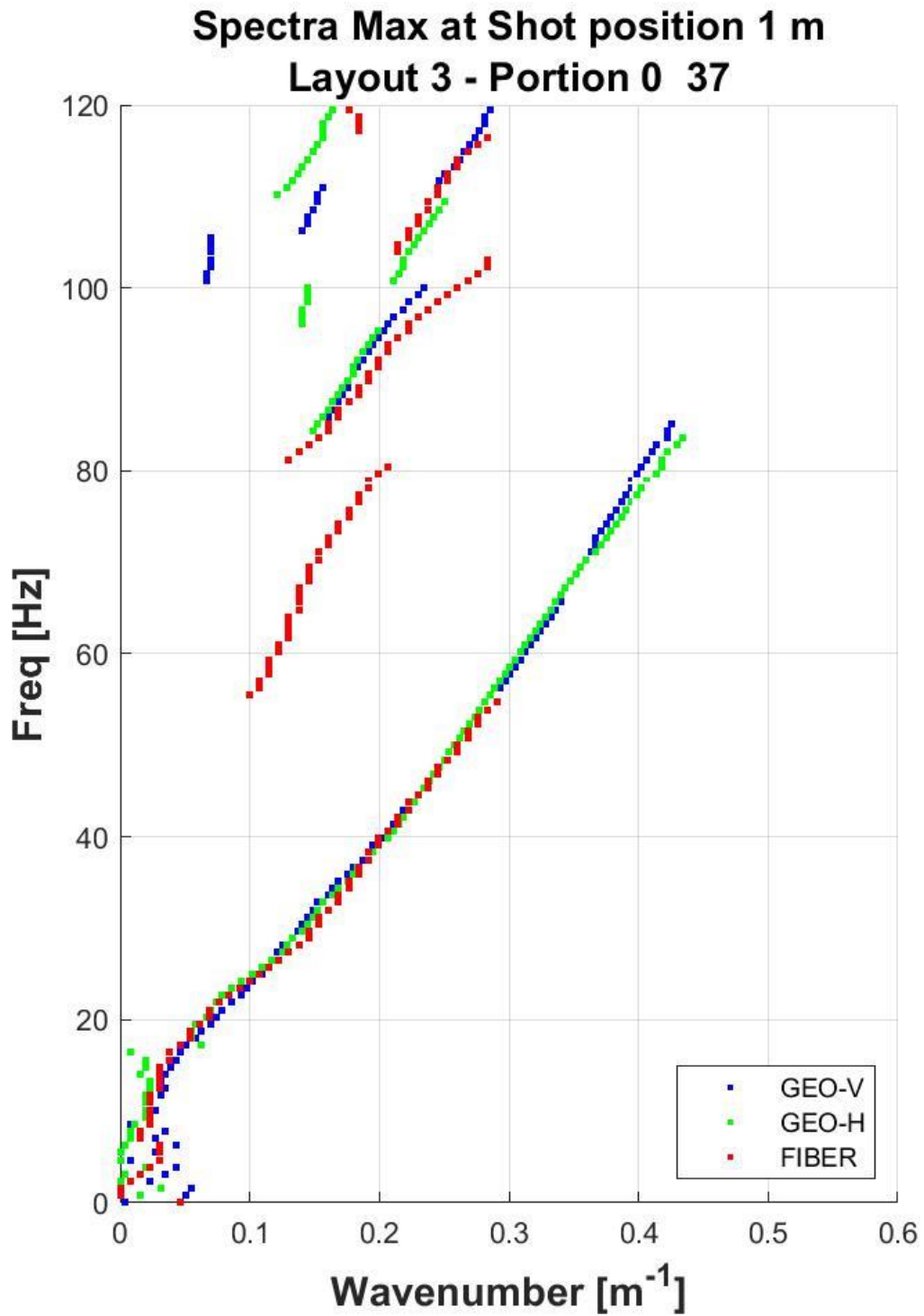


Figure 4.2.8. Comparison of the modes of propagation between vertical geophones (blue dots), horizontal in-line geophones (green dots) and fiber optic sensors (red dots). These data are extracted from an external shot of Layout 3 (0.5 m geophone spacing) in the portion of stabilized soil.

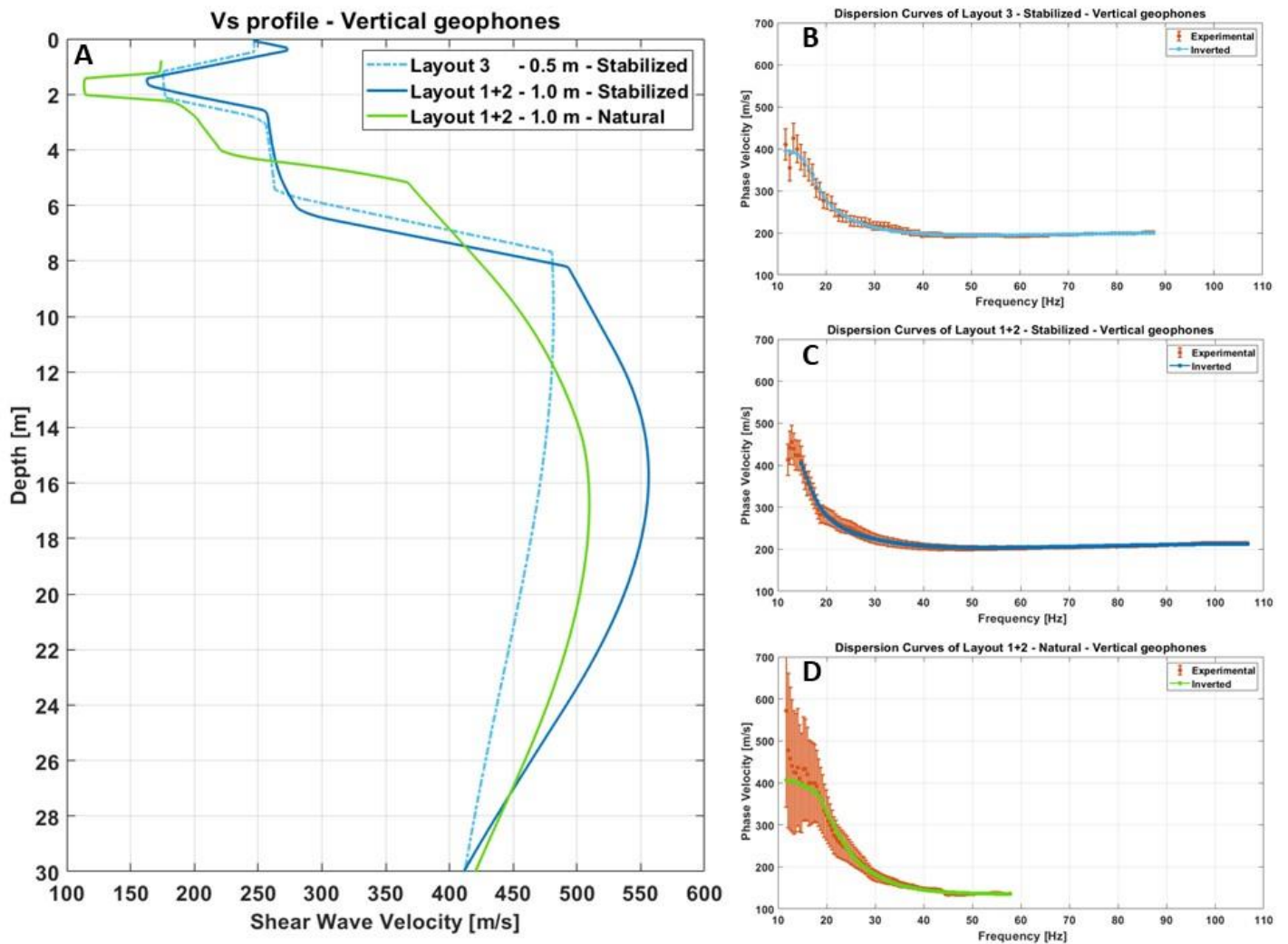


Figure 4.2.9. Result of the geophysical inversions as vertical profiles of shear-wave velocities (A) and the corresponding experimental and modelled dispersion curves for: an external shot of Layout 3 in the portion of stabilized soil (B), the combination of Layout 1 and 2 in the portion of stabilized soil (C), the combination of Layout 1 and 2 in the portion of natural soil (D).

The acquired seismic data have been analyzed also for processing through the seismic refraction method, which is a standard application for estimating the distribution of compressional wave velocities (V_p). A clear refracted event is recognizable in the acquisition of vertical geophones, while it is very weak in the seismogram of horizontal in-line geophones, hardly detectable in 20-30 m from the source (Fig. 4.2.10). The seismogram from DAS acquisition does not show any refracted event, not even characterized by a weak signal. In Fig. 4.2.10 the picked refracted event from the GEO-V seismogram is superimposed on the other two datasets. It is evident that no signal is present at those time-locations along the fiber optic data but merely high frequency noise.

The refracted waves come up to the surface with a high angle of incidence, due to the slower shallower layer. The consequence is that the wave front hits the fiber optic cable with a direction

that is almost perpendicular to the cable itself. As reported in section 2.1.1, DAS is mainly sensitive to P-waves that propagate along the same direction of the cable (small incident angles), resulting in an unobservable refraction event.

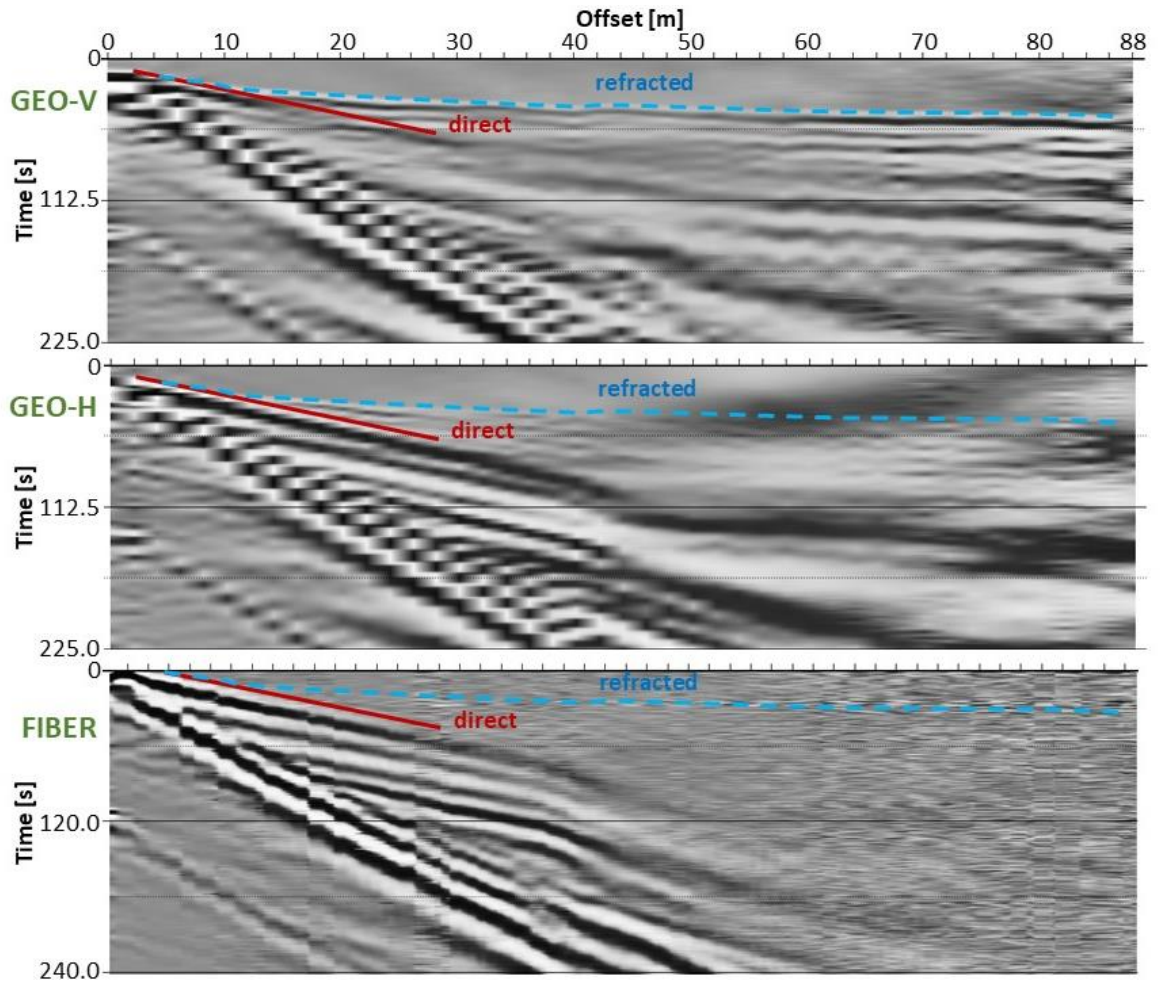


Figure 4.2.10. Seismograms from Layout 1 (2 m geophone spacing) of (from top to bottom): vertical geophones (GEO-V), horizontal in-line geophones (GEO-H) and fiber optic sensors (FIBER). Direct and refracted waves are highlighted by solid red lines and blue dashed lines, respectively.

4.3 Pile experiment

The test along a reinforced cement pile has been designed to explore capabilities and limitations of fiber optics as acoustic sensors in an extreme case. The pile theoretically represents the furthestmost case of a narrow volume of stabilized soil, where only cement binder is used. The acoustic wave velocities and the resonance frequencies are pushed towards the upper limits that might be found in a material stabilized through soil mixing.

The measurements took place on the intact pile and on the pile with artificial damages. A vertical cut has been executed in the pile, at 5 m from the source on the elongated upper side, with an increasing depth from 2 to 12 cm, in steps of 2 cm (Fig. 4.3.1). The aim is to simulate different grades of discontinuities. It was not possible to have a deeper cut without damaging the metal armor and fiber optic cable. As the last stage of simulated damages, the pile has been lifted from one side and let it fracture under its own weight (Fig. 4.3.1).

To take the advantage of the spatial sampling of DAS, we installed the cable covering two of the elongated sides (Fig. 3.4.2 and Fig. 4.3.2 A). Figures 4.3.2 B and C show the unprocessed raw seismograms. The traces recorded at position 0 and 28 m indicate where the fiber optic cable gets into the pile and they are the closest to the source; while the traces placed at around 14 m record acoustic waves located at the opposite end of the pile. These seismograms show thus a symmetry along the offset, with the wave that propagates from positions 0 and 28 m towards offset 14 m and then echoes back repeatedly between the pile extremities until the signal is totally dissipated. It is evident that the signal has reflections also from the damaged zone in the middle of the fractured pile (Fig. 4.3.2 C).

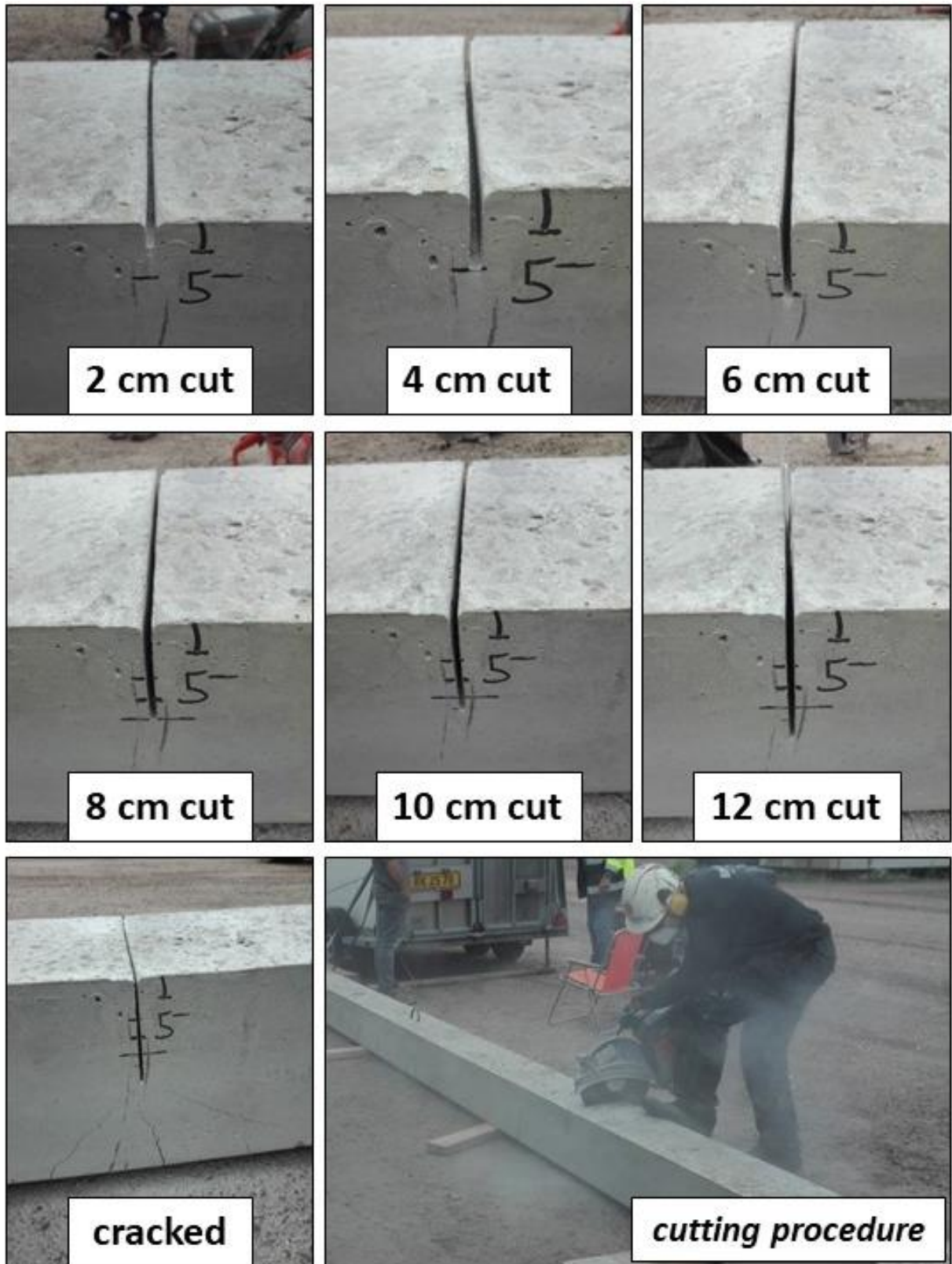


Figure 4.3.1. Photographic documentation of the simulated damages in the pile: a vertical cut progressively deepened of 2 cm steps from 2 to 12 cm. At the last stage the pile has been lifted from one side and let crack under its own weight.

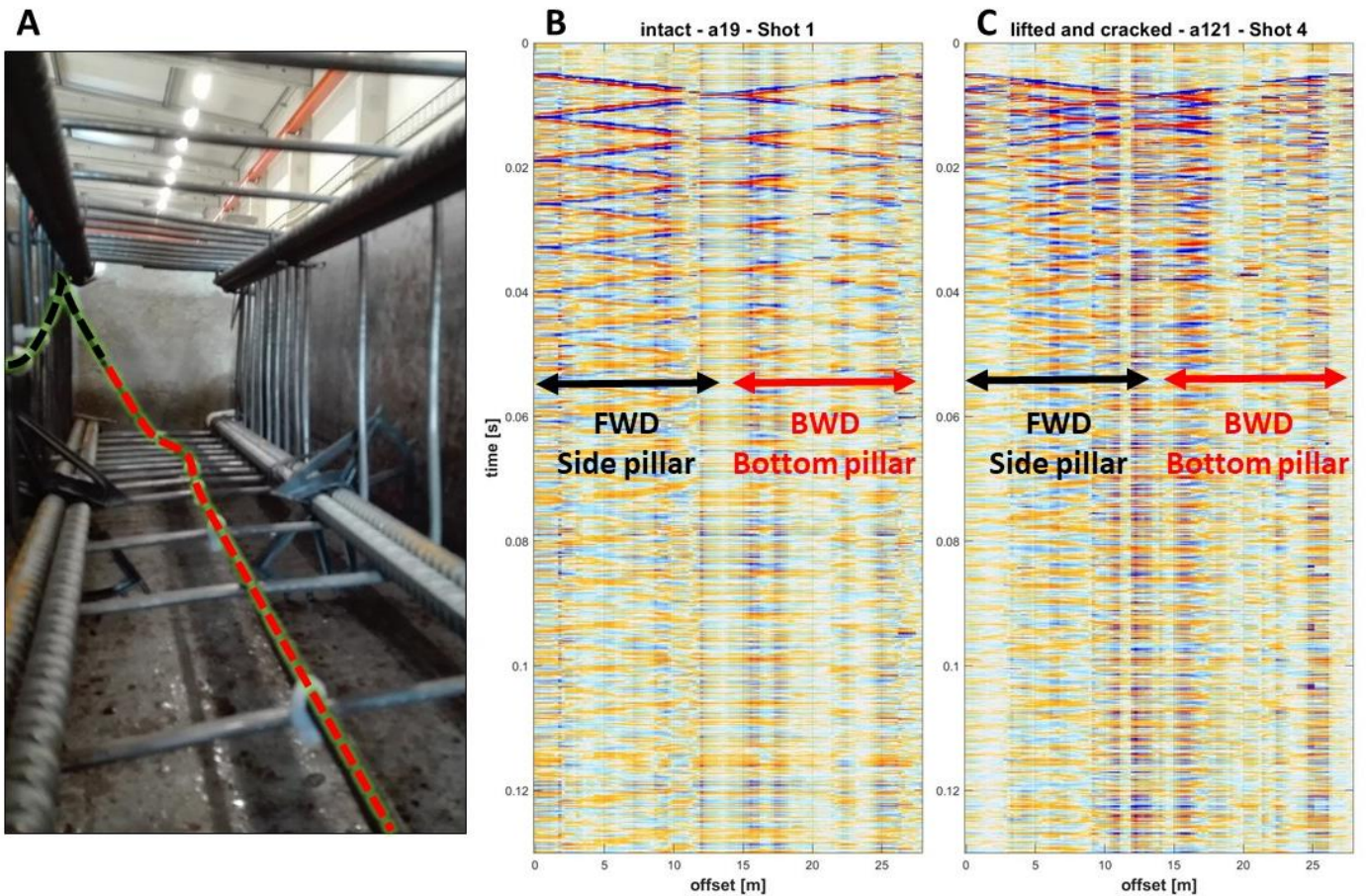


Figure 4.3.2. Raw seismograms from fiber optic sensors. A) Position of the fiber optic cable in the pile with the marked separation of lateral and bottom sides. B) Unprocessed seismogram of the “intact” pile. C) Unprocessed seismogram of the “cracked” pile.

For the sake of comparison, we extracted the two traces of fiber optic data, around 0 and 28 m, that are the closest to the accelerometer position. Fig. 4.3.3 and Fig. 4.3.4 display the traces and the relative frequency spectra for the uncut pile and the fractured material. All the traces acquired on the intact pile (Fig. 4.3.3) are characterized by distinct echoes, which occur with a constant interval of about 0.007 s, characterizing the material with an acoustic wave velocity of 4000 m/s ($V=2L/dt$). The pattern of fiber optic traces is similar to the accelerometer data, but it shows less dumping in the signal amplitude over time.

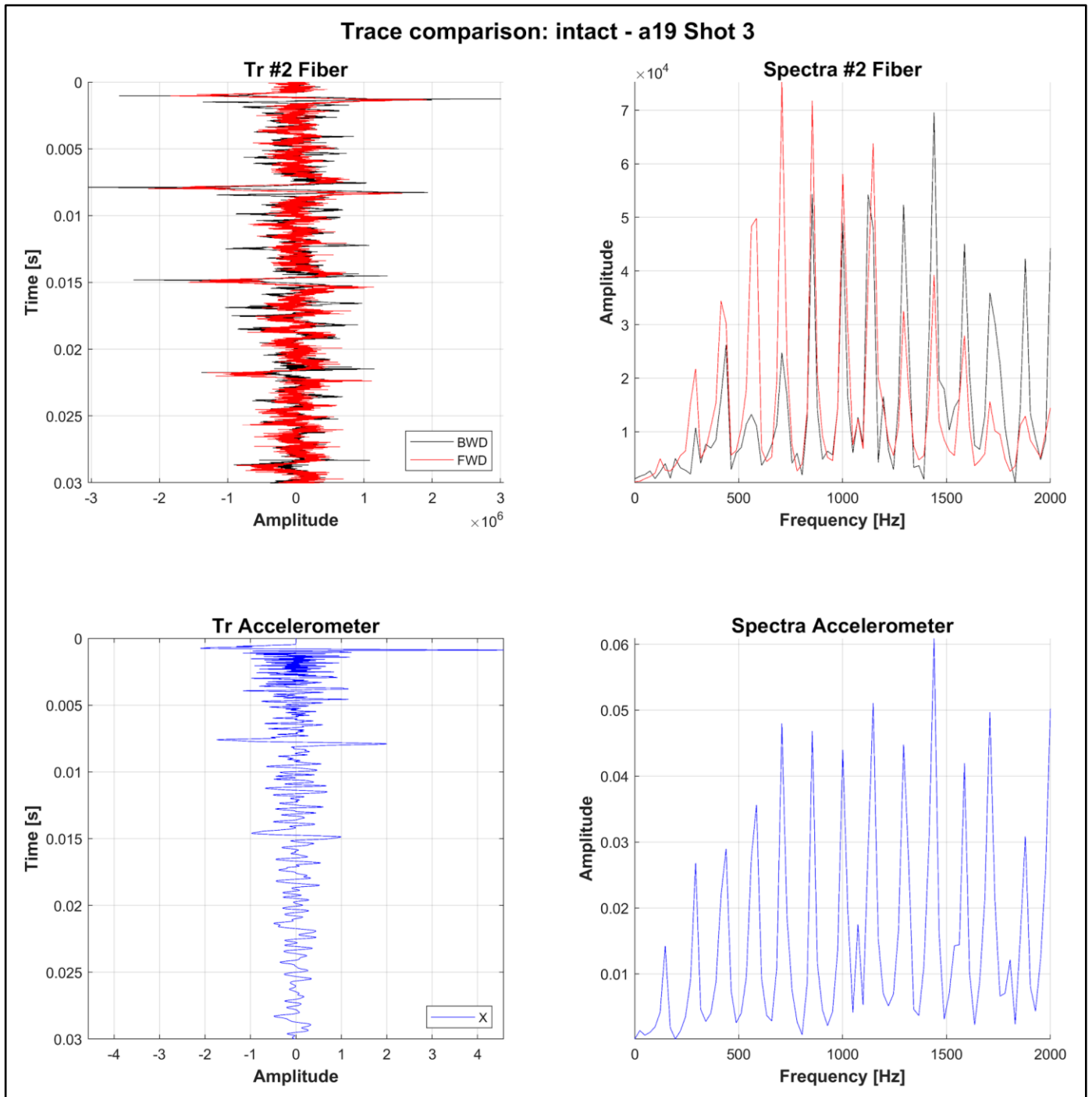


Figure 4.3.3. Test on the intact pile. The left subplots show traces acquired with DAS (red, at 0 m offset; black, at 28 m offset) and accelerometer (blue). The right subplots display the corresponding frequency spectra. Note the different amplitude scale between the two techniques, which result in different magnitudes of the spectra.

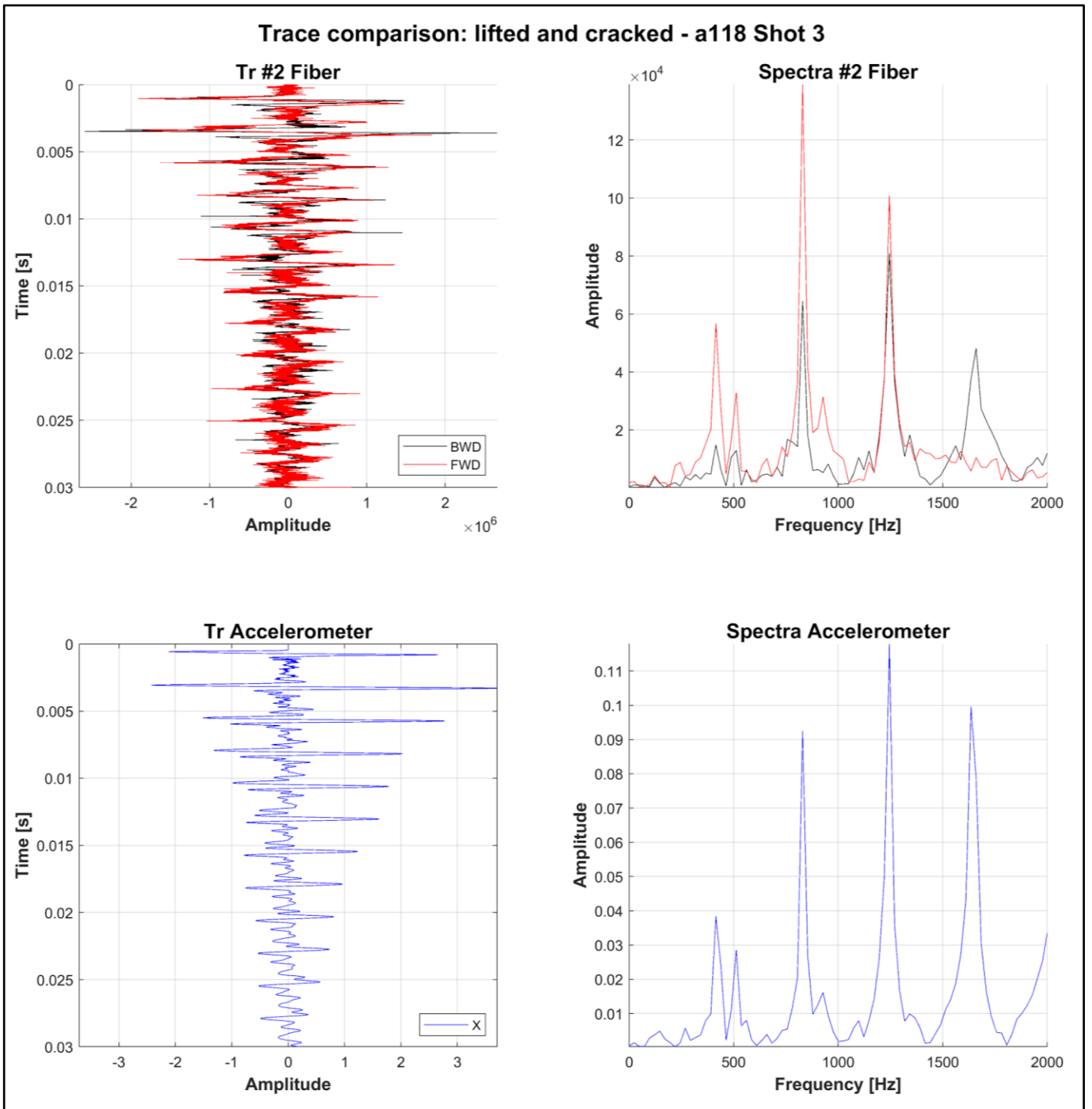


Figure 4.3.4. Test on the fractured pile. The left subplots show traces acquired with DAS (red, at 0 m offset; black, at 28 m offset) and accelerometer (blue). The right subplots display the corresponding frequency spectra. Note the different amplitude scale between the two techniques, which result in different magnitudes of the spectra.

The same considerations apply to the test on the fractured pile (Fig. 4.3.4), with the difference of the recurring time of the echoes that come about every 0.0025 s. This perfectly coincides with the position of the artificial damage at 5 m from the source, considering the acoustic wave velocity of 4000 m/s as estimated from the intact pile.

The spectra of Fig. 4.3.3 and Fig. 4.3.4 show a similar behavior between the traces recorded by the different techniques. We identify the main picks of the spectra appearing at the same frequencies, even if the magnitude is on different scales, due to the different signal amplitude recorded by the instruments. Analyzing the spectra, it is evident the discrepancy in frequency content between the uncut pile (Fig. 4.3.3) and the damaged structure (Fig. 4.3.4).

Fig. 4.3.5 displays the spectra of DAS and accelerometer data in a single plot, where the magnitude is normalized on the maximum value for each technique, with the aim of having a more direct comparison. It is clearly evident that the picks of higher energy are located at the same frequencies, even if the normalized amplitude differs. The accelerometer data show an energy distribution focalized mainly in the lower frequencies (up to 1500 Hz), while the fiber optic sensors register also higher frequency contents (up to 2500 Hz) and their higher peaks are positioned above 1000 Hz. This is a general consideration of the acquired datasets, even if it has to be mentioned that the fiber optic data show slightly different behaviors in the amplitude of the spectra when we consider traces located in other positions along the pile. This aspect is well summarized in Fig. 4.3.6, where all the DAS traces along the pile are considered. The seismogram acquired on the uncut pile is divided in two portions: forward (FWD), from offset 0 to 14 m, and backward (BWD), from offset 14 to 28 m. BWD is flipped compared to Fig. 4.3.2, to maintain the source position on the left side of the seismogram and assure a more straightforward comparison. Analyzing the FX plots of Fig. 4.3.6, it is evident how the magnitude of the spectra is varying with the offset for a certain frequency pick. Another relevant consideration about the FX spectra is the presence of segments that are affected by analogue amplitudes for a specific frequency. These segments have a length that varies from 2 to 4 m. This aspect is related to the 2 m resolution of the fiber optic sensors (Table 3.4.1), that is also visible in the seismograms (TX plots) of Fig. 4.3.6 and it appears as “horizontal steps” of about 2 m length. The signal integration on a segment that is longer than the spatial sampling interval results in an artificial smearing of the higher amplitudes along the fiber optic cable. The same behavior is prominent also in the FK plots (Fig. 4.3.6), where the energy picks for different frequencies involve a segment of about 0.2 m^{-1} as wavenumber.

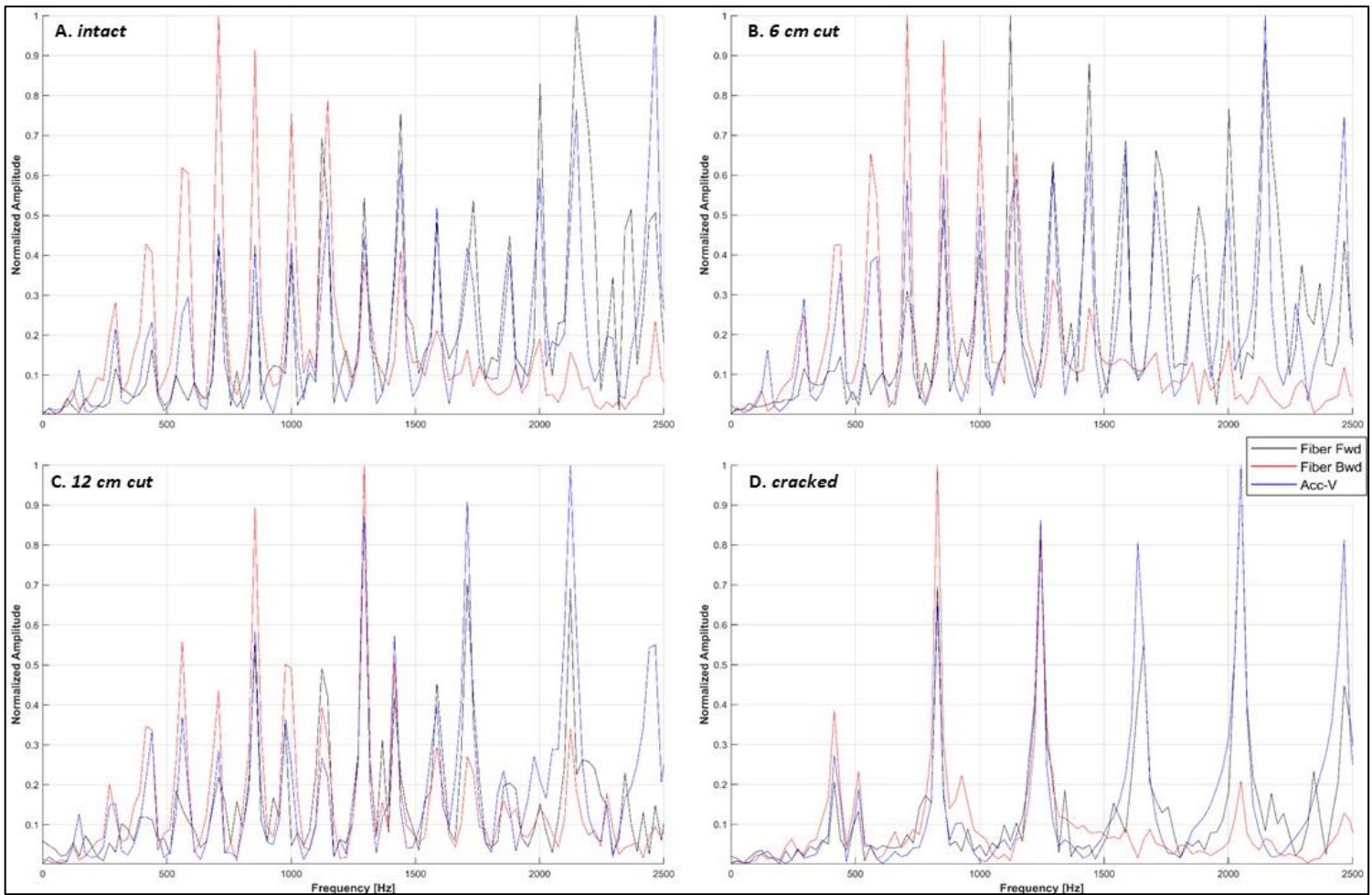


Figure 4.3.5. The spectra from the DAS (FWD, black, at 0 m offset; BWD, red, at 28 m offset) and the accelerometer (blue) are normalized for the maximum amplitude and compiled in a single plot. Results from different levels of damage: A) intact pile; B) cut of 6 cm in the pile; C) cut of 12 cm in the pile; D) fractured pile.

Fig. 4.3.6 clearly shows that the energy is distributed along the pile with a mode of propagation that involves only specific frequencies and wavenumbers (particularly evident in the FK plots). The pile vibrates with peculiar wavelengths associated with specific frequencies. This information cannot be achieved by traditional single-point accelerometer soundings and it can be highly relevant to infer and monitor the integrity of infrastructures and stabilized soil pillars.

The data acquired at different simulated grades of damage do not show relevant differences in the spectra until the cut in the pile reaches 12 cm of depth (Fig. 4.3.5 and Figure 4.3.7). The normalized amplitudes of the test with 12 cm cut display a different distribution that is characterized by 5 higher peaks that almost double the amplitude of the other peaks. Those spectra resemble the spectra of the fractured pile, even if the maxima have a slightly different frequency content. The seismograms show a distinct discrepancy only in the fractured pile, where echoes occur with shorter travel times, while no evidence is detectable in the test with 12 cm cut.

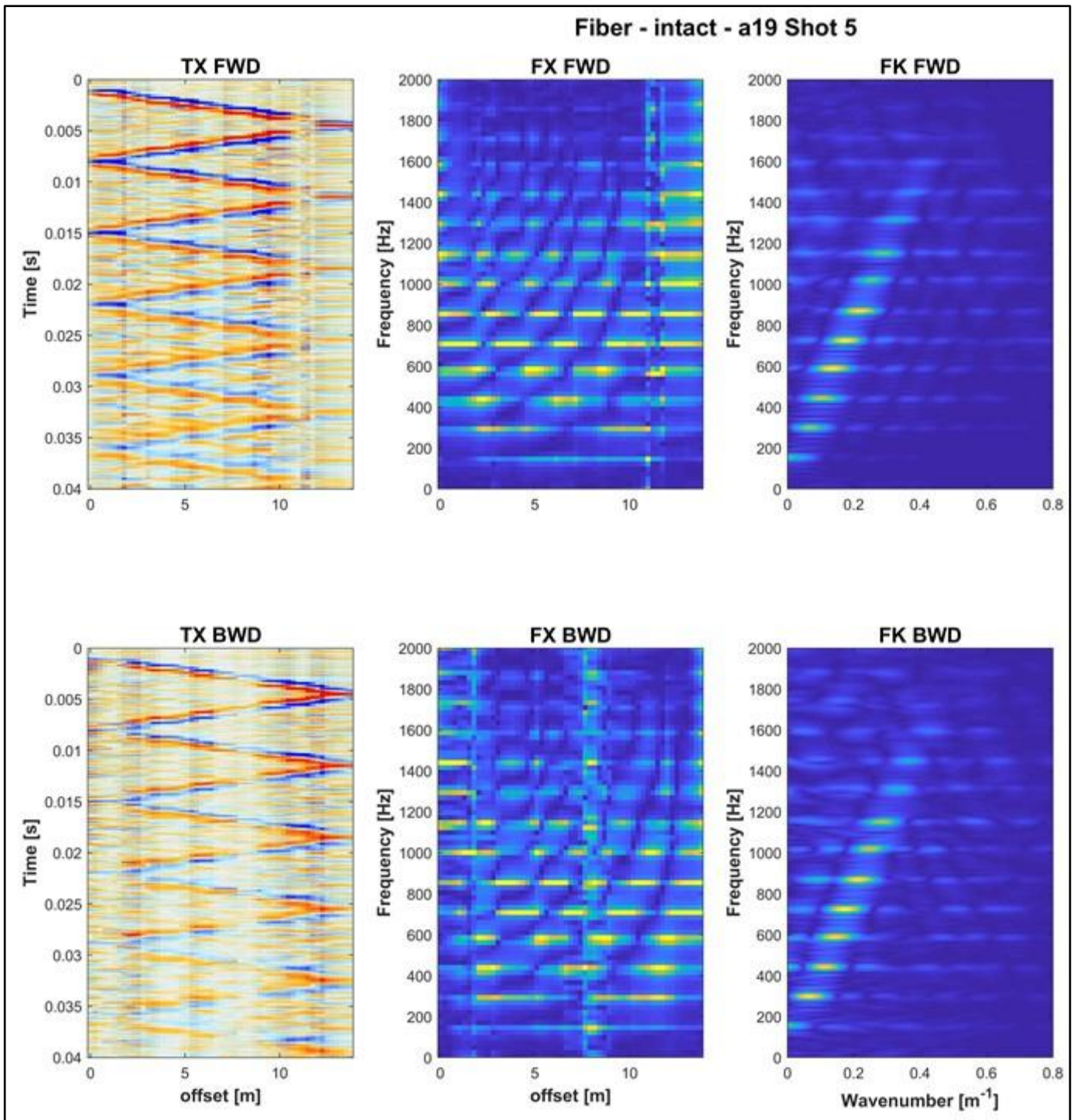


Figure 4.3.6. Fiber optic data along the entire cable length for the test on the intact pile, divided in forward (side of the pile, FWD) and backward (bottom of the pile, BWD): left column, seismograms (TX); middle column, spectra along the cable length (FX); right column, two-dimensional spectra (FK).

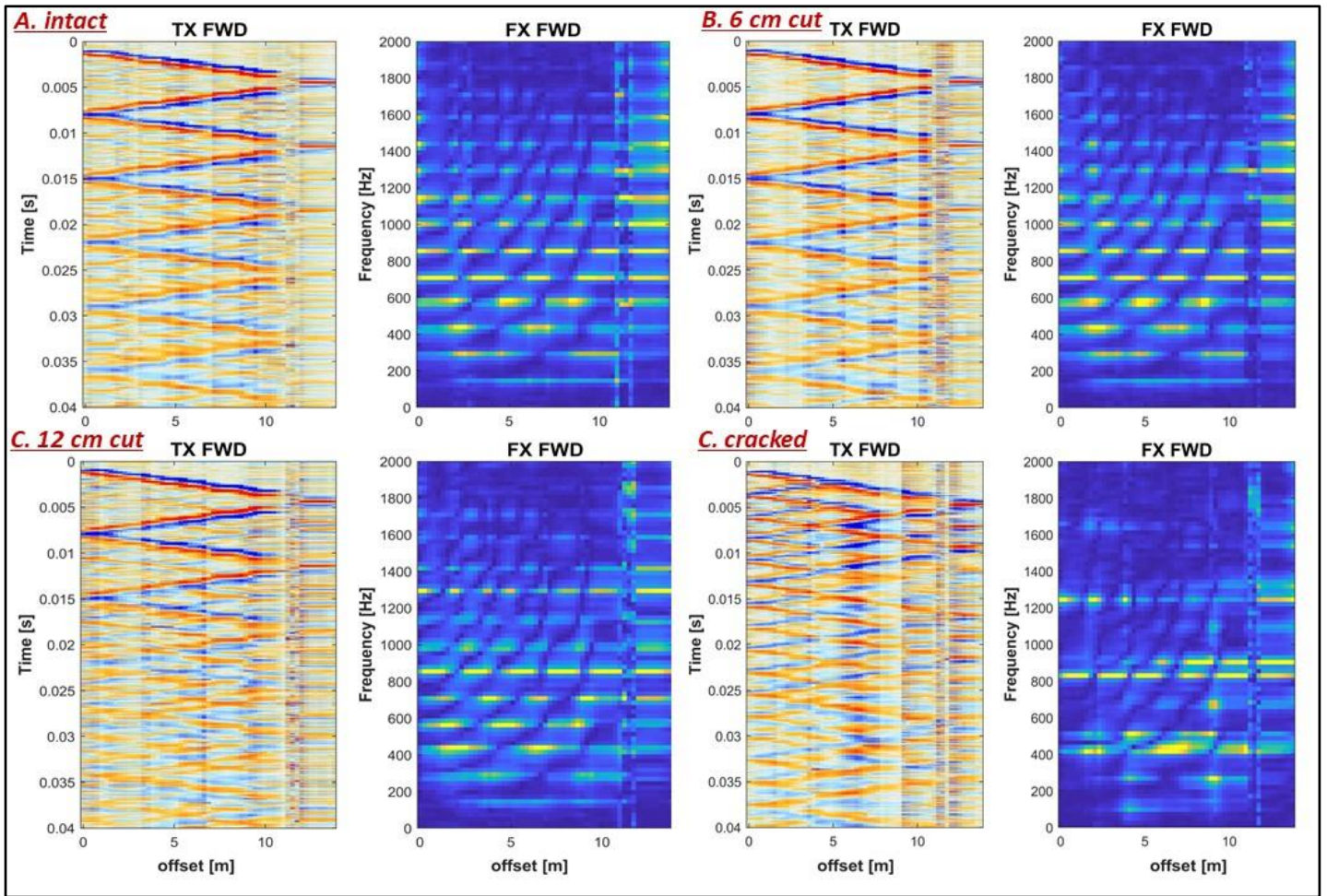


Figure 4.3.7. Fiber optic data along the entire lateral side of the pile (FWD) for different simulated damages: left columns, seismograms (TX); right columns, spectra along the cable length (FX).

5. CONCLUSIONS

The present project is a feasibility study on the application of fiber optics as acoustic sensors for civil engineering investigations in connection with soil stabilization. To verify the applicability of DAS in such a context, the projects focused on the comparison with standard acoustic sensors (geophones and accelerometers).

The results clearly show that the signal from the fiber optics can be an alternative to standard seismic receivers. As a general conclusion, DAS is a methodology that can prove a powerful tool for near-surface geophysical studies in environmental and civil engineering applications.

The signal from the fiber optics is analogue to standard seismic receivers. Fiber optics sensors display a higher similarity with the horizontal in-line component of the geophones, as it was expected, since they record the stretching of the fiber (see also Wu et al., 2017). This means that they are more sensitive to acoustic waves that propagate along the fiber than perpendicularly to the fiber.

Despite the fact that we used a DAS system that is probably the most advanced available on the market, the outcome is that the fiber optic sensors are less sensitive to smaller wavelengths compared to short-spacing geophones. This is mainly due to the 2 m resolution (Gauge length) of the applied technique. It has to be mentioned that seismic surveys are rarely conducted with an intra-geophones spacing of less than 1 m. The uncertainty of the relative location of the receivers, especially on a rugged topographic surface, usually makes traditional seismic measurements impractical with a spatial resolution smaller than 0.5 m. On the other hand, the exact location of the receiver position along the fiber optic is a great advantage of the DAS acquisitions. If further developments in the DAS systems are able to decrease the Gauge length, seismic measurements via fiber optics might have greater potential for environmental and civil engineering applications.

In spite of the limit to 2 m spatial resolution, the test along a concrete pile shows the possibility of recording high frequencies. The cause should be attributed to the fact that the pile has its own modes of vibrations that only involve high frequencies and short wavenumbers. Another reason could be the excellent and uniform coupling of the fiber optic cable within the concrete material. In this specific case, the resolution plays a role only if we look at the distribution of the signal along the cable, but it seems to not affect the single traces that are in perfect agreement with the reference measurements via an accelerometer.

Analyzing the extreme case of the pile test, the authors are confident that the method should also work for investigating other kinds of infrastructures for soil stabilization (i.e. soil-mixing pillars). The great advantage of DAS soundings along piles and pillars is the dense spatial distribution of the sensors that makes it possible to detect the modes of propagation for a large range of frequencies and wavelengths. On the contrary, traditional accelerometer surveys are conducted only on the side of the infrastructure that emerges from the ground. In this context, DAS applications can provide more accurate data and have the possibility to establish a long term monitoring of the stabilized soil.

The specifics of the instrument applied in the project (spatial resolution of 2 m and spatial sampling interval of 0.255 m) are probably the minimum requirements for these types of engineering applications. Considering that DAS is a recent development of the technology, this limit could be improved in the future, opening DAS applications to a broader range of testing and monitoring of infrastructures.

6. ACKNOWLEDGEMENTS

The authors of the report thank:

- Vinnova, SBUF and BeFo for the financial support
- The partner of the project Hydroresearch AB and Silixa ltd for supporting and showing flexibility modifying the plans of the project.
- The project partner Peab AB for funding through SBUF and the availability and support with the test on the pile.
- The project partner Skanska Sverige AB for the availability and the great support on the ESS construction site.
- The project partners SGI and NCC for the active role in the reference group.
- Impakt Geofysik AB for the availability and support with the tests made at the ESS site.
- Associate Professor Giulio Vignoli (Department of Civil and Environmental Engineering and Architecture, University of Cagliari, Italy) for providing high quality inversions of seismic surface waves obtained via a proprietary inversion code.

7. REFERENCES

Lin C.-H., Lin C.-P., Dai Y.-Z. & Chien C.-J. (2017) Application of surface wave method in assessment of ground modification with improvement columns. *Journal of Applied Geophysics*, 142, 14–22.

Lindh P. (2016) Utvärdering av stabiliserad grundläggning med hjälp av kärnprovtagning och crosshole teknik, SBUF, Stockholm, rapport id 13152, 33p.

Parker T. R., Gillies A., Shatalin, S. V. & Farhadiroushan, M. (2014) The intelligent distributed acoustic sensing, *Proc. SPIE*, vol. 9157. p. 91573Q–91573Q–4.

Rydén N. och Lindh P. (2015) Oförstörande provning av jetpelare, SBUF, Stockholm, rapport id 12841, 32p.

Vignoli, G., Guillemoteau, J., Barreto, J., Rossi, M. (2021). Reconstruction, with tunable sparsity levels, of shear-wave velocity profiles from surface wave data, *Geophysical Journal International*, (accepted) ggab068, <https://doi.org/10.1093/gji/ggab068>.

Telford, W., Geldart, L., & Sheriff, R. (1990). *Applied Geophysics* (2nd ed.). Cambridge: Cambridge University Press. doi:10.1017/CBO9781139167932

Wu, X., Willis, M.E., Palacios, W., Ellmuthaler, A., Barrios, O., Shaw, S., Quinn, D., (2017) Compressional- and shear-wave studies of distributed acoustic sensing acquired vertical seismic profile data. *The Leading Edge*, 36-12, 987-993.